THE USE OF ELECTROTHERMAL ATOMIZATION - ATOMIC ABSORPTION SPECTROSCOPY IN THE DETERMINATION OF SELECTED LANTHANOID ELEMENTS.

Janice Haines

A Dissertation Submitted to the Faculty of Science,
University of the Witwatersrand, Johannesburg,
for the Degree of Master of Science.

Johannesburg, 1985

DECLARATION

I declare that this dissertation is my own work.
It is being submitted for the degree of Master of Science
in the University of the Witwatersrand, Johannesburg.
It has not been submitted before for any degree or
examination in any other University.

Janice Haines

J. Haines

DECLARATION

I declare that this dissertation is my own work.
It is being submitted for the degree of Master of Science
in the University of the Witwatersrand, Johannesburg.
It has not been submitted before for any degree or
examination in any other University.

Janice Haines

J. Haines

ACKNOWLEDGEMENTS

This study was undertaken in the Analytical Science Division of the Council for Mineral Technology (MINTEK).

I would like to thank:

The management of MINTEK for permission to undertake the project;

Professor R.A. Hasty for his guidance and assistance during the course of this research;

Doctor John Watling for his invaluable help and moral support.

Doctor Colin Logan for his help with the X-Ray Diffraction work.

Basil Eddy for helping with the Neutron Activation Analysis.

Elaine Jones and Gerda Russell for help with the analysis of samples.

All friends at MINTEK who offered moral support especially Elspeth, Elaine, Kathy, John and countless others.

CONTENTS

LIST OF FIGURES

LIST OF TABLES

CHAPTER 1

INTRODUCTION AND THEORY

1.1) INTRODUCTION

According to IUPAC convention[1] the group of elements from atomic number 57 to 71 (lanthanum to lutetium) are defined as the lanthanoids or lanthanoid elements. If the elements scandium and yttrium are included with this group then they are known as the rare earth elements. In this dissertation the term lanthanoids (or lanthanoid elements) will be used for the group of elements from lanthanum to lutetium and rare earth elements for the group including the lanthanoids and scandium and yttrium.

The lanthanoid elements are gaining importance in many fields of application[2]. One of the major applications is the addition of these elements to various steels to increase oxidation resistance or mallesbility. Gadolinium, samarium, europium and dysprosium are used in the nuclear industry. The lanthanoids are important in the glass industry as polishing compounds and as colouring agents. Other uses of the lanthanoids include carbon arc lighting, TV tubes, garnets, hydrocarbon catalysts, and in the manufacture of very small magnets for the semiconductor industry.

Their relative abundances in the lithosphere are quite high (see Table 1) and they can be separated from each other using such techniques as fractional crysallisation, liquid-liquid extraction or by ion exchange chromatography[3].

Several analytical techniques are available for the measurement of the lanthanoid elements including inductively coupled plasma atomic emission spectrometry (ICP AES), X-ray fluorescence spectrometry (XRFS), mass spectroscopy (MS), ion chromatography (IC) and atomic absorption spectroscopy (AAS) using flame atomization or electrothermal atomization (ETA).

Atomic absorption spectroscopy (AAS) has been used for nearly thirty years as an analytical tool. The introduction of electrothermal atomization (ETA) improved the detection limits for

Table 1 : Comparison in Crustal Abundances between the Rare Earth Elements and some other Elements[6].

Element	Abundance µg/g	Element	Abundance µg/g
Lanthanum	18.3	Nitrogen	46.3
Cerium	46.1	Tin	40.0
Praseodynium	5.53	Niobium	24.0
Neodynium	23.9	Cobalt	23.0
Promethium	4.5×10^{-20}	Lead	16.0
Samarium	6.47	Gallium	15.0
Europium	1.06	Molybdenum	2.5-15
Gadolinium	6.36	Beryllium	6
Terbium	0.91	Arsenic	5
Dysprosium	4.47	Uranium	4
Holmium	1.15	Boron	3
Erbium	2.47	Tantalum	2.1
Thullium	0.20	Bromine	1.62
Ytterbium	2.66	Antimony	1
Lutetium	0.75	Iodine	0.3
		Cadmium	0.15
Scandium	5	Selenium	0.09
Yttrium	28.1	Gold	0.005

Table 2 : Comparison of Detection Limits in the Graphite Furnace and Flame Atomic Absorption Spectroscopy.[4]

Element	Detection Limits graphite furnace ($\mu g/l$) (sample size 100 μl)	Detection Limits flame ($\mu g/l$)
Aluminium	0.02	20
Arsenic	0.1	150
Barium	0.5	10
Bismuth	0..	3
Calcium	0.01	1
Cadium	0.001	2
Chromium	0.1	3
Cobalt	0.05	10
Gallium	0.1	100
Indium	0.1	20
Molybdenum	0.03	20
Lead	0.02	10
Tin	0.1	20
Titanium	20	50
Vanadium	1	50
Zinc	0.0005	1

most elements by up to three orders of magnitude. In Table 2, a comparison is made between flame and furnace atomization for several elements. A similar increase in sensitivity can be expected for the measurement of the lanthanoids using furnace atomization. This increased sensitivity should allow measurement of the lanthanoids at lower concentrations than normally attained by other techniques.

1.2) AIMS OF INVESTIGATION.

The aims of this investigation are defined and detailed below.

1) To determine the applicability of electrothermal atomization to the measurement of the lanthanoid elements and to determine optimum atomization conditions for these elements.

2) To investigate a selected group of the lanthanoids in more detail with respect to the atomization processes in the graphite furnace.

3) To investigate interelement interference effects on this group of lanthanoids and postulate interference mechanisms and hence determine methods of overcoming these interference effects.

4) To develop an analytical method for the determination of individual lanthanoids in a mixed lanthanoid matrix.

1.3) CHEMISTRY OF THE LANTHANOIDS.

1.3.1) Occurrence and Distribution[5,6,7,8].

The rare earth elements are widely distributed in low concentrations throughout the earth's crust. They occur in many massive rock formations e.g. basalts, granites, gneisses, shales and silicate rocks in the 10 to 300 $\mu g/g$ concentration range. There are also 130 discreet rare earth containing minerals most of which are rare but some have high rare earth contents in the per cent range.

The term "Rare Earths" originated from the occurrence of these elements in oxide (originally called earth) mixtures. They are not rare elements since their absolute abundances in the lithosphere are relatively high. The crustal abundancies of the rare earth elements

and
are detailed in Table 1, the abundancies of some more common elements are included for comparison. Examination of this data shows that a number of elements normally considered to be common are actually less abundant than some of the rare earth elements.

Many rare earth containing minerals have been described but only a limited number are both sufficiently concentrated in workable deposits and have significantly high enough rare earth concentration to be of economic interest. The major rare earth containing minerals are bastnaesite ($(Ce)CO_3F$), monazite ($(Ce)PO_4$), xenotime ($(Y)PO_4$), gadolinite ($(Y)M_3Si_2O_{10}$ where M= Fe or Be) and samarskite ($R^1_3R^2_2(Nb,Ta)_6O_{21}$ where R^1 = Fe, Ca etc. and R^2 = rare earth elements). The rare earth elements are also present in minerals such as calcite ($CaCO_3$), fluorite (CaF_2), the apatites ($(CaF)Ca_4P_3O_{12}$ and $(CaCl)Ca_4P_3O_{12}$) and scheelite ($CaWO_4$). The latter group of minerals do not contain the rare earth elements in sufficiently high quantities for them to be commercially viable. However the large scale conversion of some of these minerals to fertilizers and other products makes the potential supply of the rare earth elements, as a by product of this process, exceptionally large. Europium because of its divalent oxidation state is often present in minerals such as certain strontianites ($SrCO_3$), titanites ($CaTiSiO_5$), potassium feldspars ($KAlSi_3O_8$) and lead apatites.

Monazite and bastnaesite are the two most important minerals commercially. Monazite is essentially a lanthanoid orthophosphate but can contain significant amounts of thorium (up to 20-30 per cent by weight ThO_2). Since monazite has a large density, the mineral is released by weathering of pegmatites to concentrate in alluvial sands. Monazite occurrences have been reported throughout the world, but minable deposits are limited to India, Brazil, South Africa, Australia and the United States. Bastnaesite is widely distributed in nature but not in significant quantities. It gained importance after a substantial deposit was discovered in a worked out goldmine at Mountain Pass, California. The mineral was originally identified in Bästnas, Sweden. It is essentially a lanthanum-cerium fluorocarbonate containing small quantities of the other rare earth elements and

virtually no thorium.

1.3.2) Properties of the Lanthanoids and their Compounds[3,5,6,9].

The metals are prepared either by metallothermic reduction or electrolytic reduction of melts. For metallothermic reduction anhydrous lanthanoid fluorides are preferred because of their stability in moist air. Reduction is usually carried out using elemental calcium, lithium or a lithium-magnesium alloy as the reductants. It is essential that both the lanthanoid fluorides and reductants are pure particularly with regard to oxygen and carbon since these elements invariably end up in the lanthanoid billet if present at the outset. The electrolytic method suffers from the same problems as the metallothermic process. It is difficult to find cell materials which are not attacked by molten lanthanoids and thereby introduce impurities into the ingot. It is also difficult to design cells that completely exclude atmospheric elements. This method works best for the lanthanoids with low melting points.

Oxygen attacks the metals very slowly at room temperature but at elevated temperatures they may ignite and burn vigorously. Dilute aqueous mineral acids rapidly convert the metals to solutions of the terpositive ions. Reactivity with water decreases with increasing atomic number. All other non-metallic elements, except the noble gases, react with the lanthanoids, particularly at elevated temperatures.

The lanthanoids all have high melting and boiling points. Vapour pressures have been established using a variety of techniques[9] and from this data it is apparent that samarium, ytterbium, thullium and europium are significantly the most volatile. Melting points[3], boiling points[3], vapour pressures[10] and heats of sublimation[3] of these elements are detailed in Table 3.

The chemistry of these elements is essentially ionic and is determined primarily by the size of the M^{3+} ion. Certain lanthanoids show +2 or +4 states but these are less stable than the +3 state. The most stable non-tripositive states are namely cerium(IV), europium(II), terbium(IV) and ytterbium(II).

Progressive contraction of the atomic radius of the lanthanoids

Table 3 : Melting points, boiling points, vapour pressures and heats of sublimation for the lanthanoids.

Rare Earth Element	Melting point °C	Boiling point °C	Vapour pressure atm.	Heat of sublimation kJ/mol
La	918	3264	1.1×10^{-69}	431.0
Ce	798	3433	2.2×10^{-68}	422.6
Pr	931	3520	5.5×10^{-57}	355.6
Nd	1021	3074	5.0×10^{-52}	327.6
Sm	1074	1794	5.2×10^{-31}	206.7
Eu	822	1529	8.4×10^{-26}	144.7
Gd	1313	3273	9.1×10^{-64}	397.5
Tb	1365	3230	4.8×10^{-62}	388.7
Dy	1412	2567	2.8×10^{-45}	290.4
Ho	1474	2700	3.9×10^{-47}	300.8
Er	1529	2868	5.6×10^{-50}	317.1
Tm	1545	1950	2.4×10^{-35}	232.2
Yb	819	1196	1.9×10^{-21}	152.1
Lu	1663	3402	1.2×10^{-68}	427.6

with increasing atomic number has a significant effect on the properties of this group of elements. The cause of this contraction is due to imperfect shielding of one electron by another in the same subshell. Proceeding from lanthanum to lutetium, the nuclear charge and the number of 4f electrons increase. The shielding of one 4f electron by another is very imperfect owing to the shapes of the orbitals so that at each increase the effective nuclear charge experienced by each 4f electron increases thus causing a reduction in the size of the entire $4f^n$ shell. The accumulation of these successive contractions is the total lanthanoid contraction. It should be noted that the decrease although steady is not quite regular, the biggest decreases occuring with the first f electrons added ; there also appears to be a larger decrease after f^7, that is between terbium and gadolinium.

Anhydrous halides are best obtained by direct combinations of the elements. Dehydration of hydrated compounds is complicated by hydrolysis to the oxyhalide species (LnOX) particularly as the temperature increases. The fluorides are very insoluble in water and are less susceptible than the other halides to hydrolytic decomposition. The other halides are so soluble that their hydrates are not easy to obtain by crysallisation and in the anhydrous form they are both hygroscopic and deliquescent. Aqueous solutions of the chlorides, bromides and iodides are readily obtained by dissolution of the oxides, hydroxides or carbonates in a solution of the appropriate hydrohalic acid in water or by direct dissolution of the anhydrous compounds in water.

Nitrates are prepared by reaction of a small excess of the oxide with nitric acid. The salts crysallise as the hexahydrates and are very soluble in water and often soluble in alchohols, esters and ketones. When heated to 850°C, the nitrates release oxygen and oxides of nitrogen and leave the lanthanoid oxide.

Anhydrous sulphates result when the oxides are heated with a small excess of concentrated sulphuric acid and the temperature is raised to 400-500°C to decompose the acid sulphates. They are hygroscopic solids which dissolve in water with the evolution of heat. Octahydrates crystallise from aqueous solution. Sulphates pyrolyse above 1000°C to leave the corresponding oxide.

The lanthanoid oxides are of the type Ln_2O_3 and are well characterized. The oxides are obtained by the ignition of the hydroxides and most salts containing oxo-anions or by direct reaction of elemental oxygen with the metals. These compounds are sparingly soluble in water and alkaline medium but dissolve readily in dilute mineral acids. They have melting points of approximately 2000°C and their boiling points are around 3500°C. The process of vaporization of the lanthanoid oxides follows one of two mechanisms, depending on whether the oxide is that of a light (lanthanum to gadolinium) or heavy (terbium to lutetium) lanthanoid[11]. The former group dissociate to the monoxide and the latter group to the metal and oxygen.

$$Ln_2O_3 \rightarrow 2LnO + O \qquad \text{Light lanthanoid oxide.}$$
$$Ln_2O_3 \rightarrow 2Ln + 3O \qquad \text{Heavy lanthanoid oxide.}$$

Other authors[12] have determined two dissociation processes for the lanthanoids.

$$Ln_2O_3(s) \rightarrow 2LnO(g) + 3O(g)$$
$$LnO(g) \rightarrow Ln(g) + O(g)$$

They postulated that for the heavier lanthanoids the second equation is the more dominant process. The use of monatomic oxygen in the above equations is in accordance with thermodynamic literature[11,12].

Hydration of the oxides to hydroxides is a characteristic property of the lanthanoids. They absorb carbon dioxide from the air to form basic carbonates. In fact, ignition in air does not yield carbonate free oxides unless the temperature exceeds 800°C.

The hydroxides (of the type $Ln(OH)_3$) are precipitated in the hydrous form by aqueous ammonia, various amines and soluble alkalies. Hydrothermal crystallization from sodium hydroxide yields the crystalline hydroxides.

Several types of carbide are known, the three most common being Ln_3C, Ln_2C_3 and LnC_2. Carbides of the Ln_3C type are known for yttrium and the samarium to lutetium group of

lanthanoids. Ln_2C_3 type carbides are known for the lanthanum to holmium group and the dicarbide is known for all the lanthanoids.

High temperature behaviour of the lanthanoid dicarbides indicates two modes of vaporization[13]. Those elements which normally exhibit the +3 or +4 oxidation state vaporize to both the gaseous metal and gaseous dicarbide under equilibrium conditions. Lanthanoids which exhibit the +2 oxidation state yield, within detection limits, only the gaseous metal. An examination of the elements in question indicates a marked difference in their vapour pressure (Table 3). The metal dicarbides which vapourize at low temperatures principally to the elements are formed from metals with high vapour pressures, while those which vapourize to both species are formed from metals with low vapour pressures.

1.4) ANALYTICAL CHEMISTRY OF THE LANTHANOIDS.

Several analytical techniques are available for the determination of the lanthanoids. Traditionally wet chemical methods such as gravimetry, titrimetry and colorimetry were used.

The introduction of instrumental methods to analytical chemistry increased the scope of analysis of the lanthanoids. Currently, they are measured using such techniques as instrumental neutron activation analysis (INAA), inductively coupled plasma atomic emission spectrometry (ICP-AES), X-ray fluorescence spectrometry (XRFS), mass spectrometry (MS), ion chromatography (IC) and atomic absorption spectrometry (AAS) using electrothermal atomization (ETA) or flame atomization. However, most of these techniques require a relatively large mass of sample. ETA-AAS has the advantage that multielement analysis can be performed on relatively small sample masses which would have significant application in the field of lanthanoid determination and was therefore used in the present investigation.

1.5) ATOMIC ABSORPTION SPECTROSCOPY.

1.5.1) Basic Principles

The technique of atomic absorption spectroscopy relies entirely

on the absorption of energy by valence electrons of ground state atoms. When the atoms are irradiated with light of the correct wavelength (i.e. that corresponding to the energy difference between the excited state and the ground state) some of the energy will be absorbed to raise the atoms to an excited state.

Consider the system :

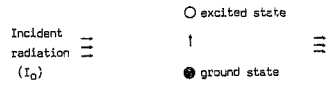

The relationship between the transmitted and incident radiation is as follows :

$$I_t = I_0 e^{(-k_\nu l)}$$

where l=absorption path length

k_ν=absorption coefficient at frequency ν.

but in spectroscopy absorbance is defined by :

$$A = \log(I_0/I_t)$$

Substituting :

$$A = k_\nu l \log e$$
$$= 0.4343 k_\nu l$$

In practical spectroscopy, k_ν is proportional to the number of atoms per cubic centimeter and hence absorbance is linearly proportional to analyte concentration, this correlation is known as the Beer-Lambert Law.

1.5.2) Basic Instrumentation.

Since the introduction of atomic absorption instruments, by Walsh in 1955[14], the analytical scope of the technique has been

extended to cover 87 elements.

Essentially an atomic absorption system consists of a light source, an atomization device, a monochromator, a detector and some form of read out[15] (see Figure 1).

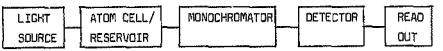

Figure 1 : Typical Atomic Absorption System.

Each of these individual components of the the atomic absorption system are discussed in detail in the following sections.

1.5.3) Light Sources.[4,15,16]

Since the energy from the light source is used to excite the valence electrons and hence give a measure of the concentration of the element under consideration, the source has several important requirements. It should produce narrow line spectra with the minimum of spectral overlap. The emission intensity of the source must be stable over long periods and ensure a low level of "noise" during analysis. The avoidance of high temperatures, pressures and current densities within the source is also an important aid to obtaining the sharpest possible spectral line. Hollow cathode lamps (HCL's) and electrodeless discharge lamps (EDL's) satisfy these conditions and are the two main types of light sources used in modern atomic absorption instrumentation.

1.5.3.1) Hollow Cathode Lamps.

The hollow cathode lamp is the most widely used light source in modern atomic absorption instruments. A diagram of a hollow cathode lamp is shown in Figure 2.

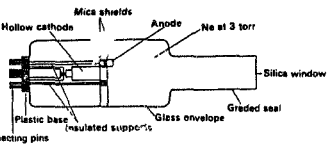

Figure 2 : Hollow Cathode Lamp[16].

The main components of this type of source are a hollow cylindrical cathode made of, or lined with the metal of interest, and an anode enclosed in a glass tube which is filled with an inert gas (usually neon or argon) at a pressure of 1 to 5 torr. When an electrical potential of approximately 500V is applied between the electrodes, a discharge of the carrier gas strikes and appears as a glowing positive column, because of the pressures used this tends to concentrate in the hollow cathode. The bombardment of these ions in the inner surface of the hollow cathode causes the metal atoms to sputter out of the cathode cup. Further collisions excite these metal atoms and a simple, intense, characteristic spectrum of the metal is obtained. Insulation helps to confine the discharge within the hollow cathode lamp and reduce the possibility of self-absorption and the appearance of ion lines, either of which can reduce the slope of the calibration curve.

Normally a different lamp is used for each element. Although multielement lamps are available, they are less satisfactory due to differing volatilities of the metals. Hollow cathode lamps have short warm-up times and a long shelf life. However for some elements, the emission intensity of the hollow cathode lamp is low and electrodeless dischage lamps are preferred.

1.5.3.2) Electrodeless Discharge Lamps.

These were first developed for use in atomic fluorescence spectroscopy.[4] Electrodeless discharge lamps (EDL's) may be operated at radiofrequencies (100kHz to 100MHz) and microwave frequencies (>100MHz). Microwave excited EDL's produce a more intense signal than hollow cathode lamps however they are much less stable.

Radiofrequency excited EDL's are less intense than microwave excited EDL's, although they are 5-100 times more intense than hollow cathode lamps. Radiofrequency excited EDL's are operated from a simple power supply at 27MHz, pretuned and enclosed to stabilize the signal. They usually have a built in starter which provides a high voltage spark to ionize some of the filler gas for initiation of the discharge. An example of a radiofrequency excited EDL is shown in Figure 3.

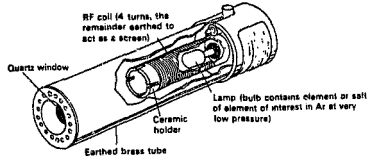

Figure 3 : Cutaway diagram of a r.f. excited EDL[16].

It is unlikely that these lamps will ever replace hollow cathode lamps in AAS since high intensity is not of paramount importance. However they have found use in replacing hollow cathode lamps with low emission intensities in which the signal-to-noise ratio (because of the low intensity of the signal) may adversely affect the detection limits[16].

1.5.4) Monochromator and Read Out Systems.[4,15,16]

Dispersion of the incident radiation so that the observer can isolate light of any particular wavelength within the range of the instrument is the classical method of wavelength separation. In modern atomic absorption instruments, gratings rather than prisms are used for dispersion. A grating is basically a transparent plate with lines ruled on it. In atomic absorption instrumentation gratings with rulings of 600 to 3000 lines per millimeter are commonly used. The grating can be mounted in the monochromator in several ways, the most commonly used are the Czerny-Turner, Ebert and Littrow systems.

Atomic absorption and atomic emission take place at the same wavelengths therefore it is necessary to discrimate between the two in order to obtain the maximum absorption signal. This was acheived in Walsh's original design where the light from the lamp was focused at the centre of the monochromator by the use of two lenses (see Figure 4).

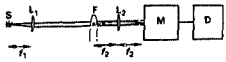

Figure 4 : Walsh type optical arrangement for AAS.[13]

The light from the lamp is focused at the centre of the monochromator by the use of two lenses. The flame is placed at the focus of the second lens so that the atomic emission signal is defocussed at the monochromator. Therefore the atomic absorption signal is maximized and the atomic emission signal minimized at the monochromator.

The next development involved placing a rotating sector (called a chopper) in the beam of light between the light source and the flame. The beam strikes a solid portion of the chopper and is interrupted, it strikes a gap in the chopper and passes through. This results in modulation of the incident radiation and the atomic absorption signal is said to be modulated but the atomic emission signal is not. An AC amplifier is then tuned to the atomic absorption signal and this selectively amplifies only the atomic absorption signal.

However this system is mechanical and can be unreliable. Consequently, most modern instruments now modulate the power supply to the light source and this may also be used to trigger the amplifier.

A photomultiplier is used as the detector in all cases. A photomultiplier tube consists of a photosensitive cathode and a series of dynodes at successively more positive potentials culminating in an anode. When photons strike the cathode, electrons are ejected and accelerated down the dynode chain. Each electron

impacting on the first dynode causes a number of secondary electrons to be ejected which are focussed on the next dynode and the process repeats itself. After suitable amplification, the signal is passed to the read out system.

The read out system can consist of an analogue or a digital meter. Many modern instruments use microprocessors to simplify interpretation of the signal and these often incorporate programs for curve correction and direct concentration read out.

1.5.5) Atom Cell or Reservoir.[4,15,16]

This is the most important component of the instrument since it is necessary to have a population of the neutral atoms of interest in order to give rise to atomic absorption.

Several forms of atom cell have been used but flames are still the most popular. Since the atom cell is required to produce atoms in the ground state, an air acetylene flame is usually sufficient to do this. However should the element under investigation form refractory compounds then the hotter nitrous oxide-acetylene flame is preferred. Pneumatic nebulization is used to introduce the sample, as an aerosol, into the flame.

Other types of atom cell include the quartz cell used for the analysis of mercury by the cold vapour technique and the analysis of hydride forming elements and the optically clear cell associated with electrothermal atomization.

1.6) ELECTROTHERMAL ATOMIZATION

1.6.1) Historical Development[17]

A.S.King is recognised as being the first scientist to investigate electrothermal atomization processes. In 1905[18] and 1908[19] he reported on fundamental spectral studies using an electrically heated tubular furnace. It was 1959 before L'vov[20] began to publish his classical work on the application of electrothermal furnace atomizers for quantitative atomic absorption

analysis. Here the sample was applied to the tip of a carbon electrode which was introduced into a cylindrical heated furnace through a transverse aperture at the centre of the tube. At first, the sample was heated using a powerful DC arc, later this was changed to simpler resistive heating of the electrode. The tube did not act as the atomizing surface, but merely as an atom cell, the sample was atomized from the electrode. The atomizer was placed within a chamber filled with nitrogen or argon and the light passed down the tube for atomic absorption measurement. This apparatus, although it gave good sensitivity, was critisised for being too cumbersome.

In 1967, Massman[22,23] described his heated graphite furnace. The graphite furnace consisted of a graphite tube with a hole drilled in it for the introduction of liquid samples. The graphite tube was supported between two water cooled steel cones which were electrically insulated from each other. The furnace was operated in an atmosphere of argon. Because of its simpler design, this device was adopted by most instrument manufacturers.

1.6.2) Graphite Furnaces.

Graphite was chosen as the standard furnace material because it has several important characteristics necessary for a good furnace material. These are :

1) Good thermal and electrical conductivity.
2) Relative chemical inertness.
3) Very low levels of metallic impurities.
4) Good machineability.
5) Low thermal expansion and high rigidity.
6) High melting point.

However graphite has two important disadvantages in that its porosity is quite high and there is a tendancy for some elements to form refractory carbides. These may be partially overcome by coating the tube with pyrolytic graphite which, because of its structure, is less porous and therefore reduces diffusion losses.

Pyrolytic coatings on graphite furnaces, usually 10μm thick, are formed on the surface of the original furnaces in a large production oven. In the manufacturing process, pyrolytic graphite is deposited on

the substrate graphite from the vapour phase after thermal decomposition of a simple hydrocarbon such as methane under low pressure. As this deposition proceeds, a dense, hard layer of pyrolytic graphite is built up over the substrate graphite. The crystals of the pyrolytic graphite lie virtually parallel to the surface and it is anisotropic, both electrically and thermally.

An alternative method of producing a pyrolytic coating on furnaces is to coat "in-situ"[23]. A 10% methane/90% argon mixture is passed through the furnace which is heated to 2000°C. The coating is formed on an electrically heated substrate rather than in an isothermal environment and this method although useful in carefully controlled circumstances, in general, gives inferior results to the commercially manufactured item.

Some workers have also used other linings[24] (e.g. tungsten or tantalum) or even metal atomizers[25] in order to reduce carbide formation. Such linings or atomizers although very useful for certain types of analysis, have several disadvantages. Their mechanical resistance may decrease after prolonged heating, their chemical resistance is lower than graphite and inter-metallic compounds can form between the surface and the analyte. Another method of reducing the reactive graphite surface is to deposit a carbide lining on the inner wall of the furnace[26] (e.g. by using tungsten, tantalum, zirconium or lanthanum salts). Several workers have reported superior sensitivities and longer furnace lifetimes for these tubes.

Recently glassy carbon has been used as an alternative to graphite. This material has the advantages of being considerably less porous than graphite and the glassy surface is resistant to chemical attack. Using standard ETA power supplies, the maximum attainable temperature of a glassy carbon furnace is 2500K but recently it has been reported[27] that with only minor modifications to the power supply, temperatures of up to 3200K can be acheived.

1.6.3) Sheath Gas.

Metal atomizers become brittle with oxidation whereas graphite atomizers become porous due to loss of carbon as carbon monoxide or carbon dioxide. Consequently electrothermal atomizers have to be

purged with an inert gas, usually nitrogen or argon, in order to reduce oxidation of the atomizer surface. Nitrogen, although cheaper than argon, can cause reduced sensitivity for some elements probably as a result of nitride formation. Therefore argon is the most often used sheath gas. The gas flows around the outside, as well as through the inside, of the graphite furnace and exits through the sample injection hole. The gas flow rate, in most modern instrumentation, is adjustable.

1.6.4) Graphite Tube Dimensions.

Initially it was thought that maximum sensitivity would be obtained from larger tubes, as these would retain the atomic vapour for a longer period. However if the furnace is too large, it attains its operating temperature too slowly and causes relative background absorption effects. Small furnaces tend to have better absorption efficiencies because focus of the radiation beam occupies a larger proportion of their measuring volume. Because of this and their shorter temperature rise times, they usually have better absolute sensitivities. Very small sample volumes, however, give rise to worse relative sensitivity and analytical accuracy. Most manufacturers offer small furnaces typically 20-30mm long and 3-5mm in diameter.

The efficiency of heating the graphite furnace is also important. The faster the heating rate, the more atoms will be formed in the atom cloud and hence the higher the sensitivity. In most commercially available graphite furnace designs electrical contact is made at the ends of the furnace by the use of metal or graphite collars. These collars are water cooled and hence their temperature never attains that of the furnace centre therefore there is a temperature gradient along the length of the furnace. All electrothermal atomizers have a common problem of non-uniform temperature distribution along the furnace length. This temperature gradient is also time dependent since it increases with increasing temperature and can reach values in excess of 1000 Kcm^{-1} for the HGA-2100 with a central temperature of 3000 K.

Temperature gradients can give rise to interference effects in the graphite furnace in two ways. Firstly by vapour condensation on

the cool furnace ends causing memory effects or more importantly by recombination and condensation of the sample vapour. These are the major contributers to spectral interferences due to molecular absorption and light scattering.

Use of miniature graphite furnaces (e.g. Varian CRA-63 and CRA-90) obviates the temperature gradient problem. It has been shown that the maximum difference in temperature from the centre of the furnce to the ends is only 240 K. In this design contact resistance heating was used which ensured localised heating and high power transfer.

1.6.5) Furnace Wall / Gas Temperature.

Critical control of the temperature program is essential in electrothermal atomization techniques. Drying and ash temperatures affect the accuracy and reproducibility of the measurement whereas atomization temperature influences the sensitivity of measurement and condensed phase interferences. Up to this stage, the wall temperature is the decisive quantity but the subsequent chemical and physical processes in the gas phase are governed by the temperature of the vapour inside the furnace and hence spectral and vapour phase interferences.

Measurements of the wall temperature are carried out quite simply with a thermocouple but vapour temperatures have to be determined spectroscopically. Vapour temperatures have been determined for the CRA-63 and HGA-2000 and 2100 furnaces[28]. These can be summarised by stating that in smaller furnaces the average vapour temperature may lag the wall temperature by 100 K and in larger furnaces by 300 K.

1.6.6) Furnace Atomization Cycle.

In electrothermal atomization the processes of drying, pyrolysis and atomization are seperated, this renders the technique with a degree of control unattainable with a flame. Most modern electrothermal atomizers are equipped with programmable power supplies which allow a wide selection of operating conditions.

However for simplicity the furnace cycle can be divided into four distinct phases :

1) Drying Stage.

This is a low temperature heating cycle required to evaporate the solvent. A temperature slightly below the boiling point of the solvent is used to prevent sputtering which would lead to irreproducible results. The drying time is established as being the time required to allow complete evaporation of solvent before the next phase and is dependant on the volume and volatility of solvent present.

2) Pyrolysis or Ashing Stage.

The objective of this stage is to remove as much of the sample matrix present as possible without significant loss of the element under investigation. This reduces interelement and background interference effects. The pyrolysis or ashing time is again dependent on the amount of sample but also on the complexity of the matrix.

3) Atomization Stage.

As well as being element dependent this stage is also matrix dependent, since the atomization process for a given element is dependant on complexes present within the sample. The atomization temperature is optimized as being the lowest temperature required to give the maximum analytical signal. The lower the temperature, the longer the lifetime of the graphite furnace. The atomization time should be the minimum required to completely vaporize the analyte i.e. the analytical signal should return to the baseline.

4) Tube Clean Stage.

If, at the end of the atomization stage, there is any residual analyte or matrix this may affect any subsequent measurements giving rise to a "memory effect". Therefore a tube clean stage is incorporated into the furnace cycle to remove as much of the residual sample as possible prior to further analysis. During this stage the temperature is increased to several hundred degrees above the initial atomization temperature.

1.5.7) Atomization Processes.

Electrothermal atomization techniques give greater sensitivity

than conventional flame techniques because of their superior atomization efficiency and the fact that the thermally produced atoms are retained for a longer period in the optical path. Thus, over this period the rate of formation of free atoms must be greater than the rate of their removal from the light path. The absorbance maximum is reached when the two rates are in equilibrium.

The processes involved in the production of these atoms are dependant upon the compounds present in the furnace, the material from which the furnace is constructed, the atmosphere within the furnace, the atomization temperature and the rate of increase in temperature.

Thermodynamic and kinetic principles have been used to explain atomization processes in electrothermal atomizers. Several possible reactions are involved :

1) Conversion of the metal salts to the oxide.

At high temperatures nitrates, sulphates and some chlorides are usually converted to oxides.

2) Evaporation of metal oxide or halide prior to atomization.

Most metal halides are volatile and evaporate before atomization. Some metal oxides have high vapour pressures at the temperature at which atomization is first observed to occur (i.e. the appearance temperature).

3) Thermal dissociation of the metal oxide.

Dissociation of the metal oxide is related to the temperature and pressure in the system and to the other species present. The degree of dissociation of the metal oxide, α , can be calculated from the following equations :

$$-\Delta G = RT\ln K_p$$

and $$\alpha = K_p/[K_p + P_{O_2}]$$

where ΔG is the free energy, P_{O_2} is the partial pressure of oxygen and K_p is the equilibrium constant for the dissociation of the metal oxide, MO as shown in the following equation :

$$MO \rightleftharpoons M + \tfrac{1}{2}O_2$$

Free energy values at various temperatures can be obtained for many metal oxides from tables of thermodynamic data.

In graphite atomizers, the value of P_{O_2} is effectively controlled by the equilibria :

$$2C + O_2 \rightleftharpoons 2CO$$
$$2CO + O_2 \rightleftharpoons 2CO_2$$

4) Reduction of the metal oxide.

For a graphite atomizer, the reduction process can be described by the following equation :

$$MO(s/l) + C(s) \rightleftharpoons M(g) + CO(g)$$

In general terms, ΔG^o_{react}, the free energy of reaction can be calculated from the free energy of the products minus the reactants. Calculation of the free energy of reaction over a wide range of temperatures, allows the estimation of the temperature at which the formation of free gaseous metal becomes feasible i.e. when ΔG^o becomes negative.

Ellingham diagrams have been used for these calculations. These diagrams were originally used for studying metallurgical processes and they require some modification to incorporate the added criterion for the f- -ation of gaseous metal atoms. In this case the thermodynamic information is presented graphically. The essential reactions to consider are :

$$MO(s/l) + C(s) \rightleftharpoons M(g) + CO(g)$$
$$C(s) + O_2(g) \rightleftharpoons CO_2(g)$$
$$2C(s) + O_2(g) \rightleftharpoons 2CO(g)$$

Such a thermodynamic approach can be extended to consider such problems as carbide formation :

$$MO + 2C \rightleftharpoons MC + CO$$

The difficulty in using a purely thermodynamic approach is that

it deals with equilibrium criteria whereas the situation in a furnace is highly dynamic. Therefore although thermodynamic considerations are important in the determination of the feasibility of atomization processes, it is apparent that these processes must also be kinetically controlled in order to explain experimental results.

L'vov[28] proposed the following equation for the atomization process taking place inside a graphite furnace. The rate of change of the number of atoms N in the gaseous state in the atomizer is the difference between the number of atoms entering the system (n_1) and the number of atoms leaving the system (n_2).

$$dN/dt = n_1(t) - n_2(t)$$

Tors[29] and Tesari[30] designed a model for a carbon rod atomizer. They assumed that the sample was deposited on the surface as a monatomic layer and that the space around the carbon rod acted as an infinite sink for evaporated atoms. The rate of release of atoms is given by :

$$n_1(t) = -sq\frac{d\theta}{dt} = ksq\theta$$

where s = surface area in cm^2

θ = the fraction of the surface covered at time t ($0 < \theta < 1$)

q = the surface concentration when $\theta = 1$

k = rate constant for the evaporation process

and $k\theta = \frac{d\theta}{dt}$.

For a normal Arrhenius temperature dependance of k

$$n_1(t) = Aqs\theta e(-\Delta G/RT)$$

where A = frequency factor constant

R = gas constant

T = temperature in degrees Kelvin

This equation describes the typical peak signal because as T

increases with time, there is a corresponding decrease in the value of θ as atoms are lost from the surface.

Fuller[31] developed a model for atomization under isothermal conditions applicable to less volatile elements in a tube type atomizer. In this case :

$$n_1(t) = k_1[N(o) - N(t)]$$

where N(o) is the initial quantity of element introduced into the atomizer
N(t) is the quantity of element atomized to time t
and k_1 is the rate constant for the atomization process

But $N(t) = N(o)[1-e^{(-k_1t)}]$

on substitution

$$n_1(t) = k_1N(o)e^{(-k_1t)}$$

The rate of atom loss is controlled by diffusion and by the flow of purge gas through the furnace. Therefore :

$$n_2(t) = k_2N$$

where k_2 is the rate constant for atom removal

Hence $dN/dt = k_1N(o)e^{(-k_1t)} - k_2N$

On integration

$$N = [k_1/(k_2-k_1)]N(o)[e^{(-k_1t)}-e^{(-k_2t)}]$$

which represents the quantity of atoms at any time.

Kinetic principles have been used to postulate reaction mechanisms in electrothermal atomization. The Arrhenius equation expresses the variation of a rate constant with temperature.

$$k = A \exp(-E/RT)$$

A graph of ln k vs. 1/T yields a straight line whose slope is equal to -E/R. Since E represents the energy required to produce metal atoms, its value may be related to the thermodynamic functions described earlier.

1.7) INTERFERENCE

Interference is defined as an effect in which there is a systematic deviation of the analyte signal in the presence of concomitants. The interference may be due to a particular concomitant or the combined effect of several concomitants. A concomitant which causes an interference is called an interferent. Interference only causes an error if not adequately corrected for during an analysis. Uncorrected interference may give rise to either enhancement or suppression of the analyte signal.

Although flame atomic absorption is subject to interference effects, usually these effects are less severe than those experienced using electrothermal atomization techniques. The superior sensitivities obtained when using electrothermal atomizers are due to the generation of higher concentrations of neutral atoms. The physical processes governing atom production can, however, also give rise to higher interferent concentrations.

According to IUPAC nomenclature approved in 1975[32], interference in both flame and electrothermal techniques can be divided into two groups :

1) Spectral interferences which can be due to incomplete isolation of the analyte signal from that of the interferent.

2) Non-spectral interference caused by changes in the atomic concentration being measured and therefore affecting directly the analyte signal.

Non-spectral interferences can then be subdivided into two distinct groups, namely condensed and vapour phase interferences. Condensed phase interference is a change in the rate of analyte supply and vapour phase interference is a change in the rate of analyte removal.

1.7.1) Spectral Interference.

This type of interference is usually the result of molecular absorption and/or light scattering by particles in the optical path.

1.7.1.1) Interference Mechanism.

Scattering of the light beam by a "fog" of molecular species at the cooler furnace ends was first noted by L'vov[29]. Apart from particles formed by condensation from the vapour phase, particles can also be formed during decomposition of organic materials or by release of graphite from the furnace at high atomization temperatures. Massman et al[34] suggested that molecular absorption spectra in the ultra violet and visible region can be divided into two groups, namely dissociation continua and electronic band spectra.

The dissociation continua which show characteristic band maxima are due to dissociation of molecules in the vapour phase following absorption of light quanta (*i.e. photodissociation*). Gucer and Massman[33] were able to follow vaporization and decomposition of molecules containing larger numbers of atoms by identifying several intermediate decomposition products. An example is the vaporization and decomposition of various metal sulphates in the graphite furnace and the ability to confirm the following photodissociation processes taking place[33,34] :

$SO_3 + h\nu \rightarrow SO_2 + O$ absorption threshold wavelength 330nm
$SO_2 + h\nu \rightarrow SO + O$ absorption threshold wavelength 190nm
$SO + h\nu \rightarrow S + O$ absorption threshold wavelength 245nm

The absorption electronic band spectra observed in graphite furnaces as with the corresponding emission spectra of molecules and radicals display fine structure and high spectral resolution instrumentation is necessary to obtain a true picture of electrothermal atomization. Prominent CN-bands have been observed in nitrogen purged furnaces, these have band heads close to 380nm and show an exponential absorbance increase as the furnace ages[33,34]. Strong C_2-bands with band heads between 430 and 570 nm have also

been suggested to contribute to furnace background.

When heated to temperatures in excess of 1000°C, the graphite furnace will emit light similar to that of a black body radiator. This emitted light is essentially dc in nature because of the thermal mass of graphite. Since most atomic absorption spectrometers modulate either the source or detector or both, this dc component is rejected even when impinging on the photomultiplier. However a level can be reached when this dc emitted component "breaks-through" the electronic system and the results will become unreliable. Several factors increase the likelihood of such event at a given furnace temperature, viz;

1) Wide monochromator bandpass.

2) Low hollow cathode lamp currents.

3) Incorrect furnace alignments.

4) Use of wavelengths in the 300-600nm regions.

5) Elements whose hollow cathode lamps are relatively weak in output.

The emission profile of graphite at 2700°C is shown in Figure 5. The ratio of emission intensity from the furnace to intensity of the hollow cathode lamp at the recommended operating conditions is greatest for the elements barium, calcium, dysprosium, erbium, europium and terbium (using their recommended atomization conditions). Therefore problems with incandescence are most likely to occur with these elements.

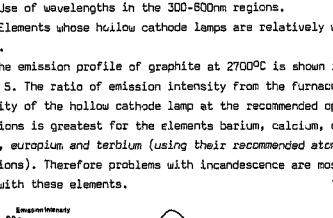

Figure 5 : Emission Profile of Graphite at 2700°C.[54]

Consequently it is important that the atomizer is properly aligned to reduce incandescence effects. Operation of the hollow cathode lamp at a higher current will enable a lower gain to be used on the photomultiplier. The use of a reduced height slit or a reduction in atomization temperature will also reduce emission intensity at the photomultiplier.

1.7.1.2) Interference Removal.

Interference can be removed or reduced by chemical or non-chemical means.

a) Interference Removal by Chemical Means.

The analyte can be chemically separated from the matrix by the use of ion exchange resins or by solvent extraction techniques. However these methods are time consuming and prone to contamination.

It is also possible to separate the analyte from the interferent, in the furnace itself, by selective volatilization. If the matrix is more volatile than the analyte, then it may be possible to remove the matrix by the use of high ash temperatures or long ashing times. Alternatively, it may be possible to atomize a significant and reproducible portion of the analyte at a temperature lower than the volatilization temperature of the matrix.

Chemical pretreatment can be used if the volatilities of the analyte and interferent are similar. It can be used in combination with or without ashing to control both spectral and non-spectral interferences. An example of this is the addition of nickel to stabilise elements like arsenic and selenium and hence allow a higher ash temperature to be used to remove the matrix. Conversely, addition of such compounds as ammonium nitrate to solutions which are high in sodium chloride, allows conversion of the matrix itself to a less volatile form.

Another special type of chemical pretreatment is the addition of reactive gases to the furnace. Hydrogen has been used considerably in the past[35,36]. Both spectral and non-spectral interferences are

reported to be considerably suppressed by the reducing environment when a hydrogen diffusion flame was burning similtaneously with analyte vaporization from the furnace. The use of a halocarbon/argon mixture has also been used to overcome refractory oxide or carbide formation in electrothermal atomization[37].

Electrodeposition has also been used as a means of separation of the analyte from the matrix. In this technique an electrochemical cell is set up and the analyte is separated by controlled potential electrodeposition onto a carbon rod[38], a hanging mercury drop[39,40] and high melting point wires of various types[41,42] are used in this procedure. The analyte is then atomized in the normal way.

The use of a constant temperature furnace may also overcome some matrix interferences since the gas temperature into which the sample is atomized is important. As described in section (1.6.1), the historical development of electrothermal atomization centred around two different types of atomizer - that of Massman (the pulse operated furnace) and that of L'vov (the constant temperature furnace). Each of these types effect the interference mechanism.

1) Pulse Operated Furnace.

Because of its simplicity, almost all commercially available electrothermal atomizers are based on the Massman design. The major limitation of this design is temporal non-isothermality which is responsible for fractional atomization. The AA signal is recorded during a time period over which the temperature of the electrothermal atomizer is rapidly changing. This situation affects the interference in two ways. Firstly, the atomization temperature for a given element cannot be practically influenced by the selection of atomization parameters and incomplete dissociation results especially for volatile elements. Secondly under temporal non-isothermal conditions, the integration method of measuring AA cannot be correctly applied.

2) Constant Temperature Furnace.

With the use of the L'vov constant temperature furnace however, the furnace attains thermal equilibrium prior to atomization of the analyte and hence much greater control of dissociation equilibria can be exercised. In practice, this system is in part affected by use of a L'vov type platform. This consists of a piece of pyrolytically coated

graphite which is placed inside the graphite furnace. The graphite furnace is heated in the normal way but the sample is atomized from the graphite platform which, because it is heated by convection, lags the furnace temperature by several degrees. The system is therefore in thermal equilibrium prior to atomization.

b) Interference Removal by Non-Chemical Means.

Background correction is essential for the removal or reduction of spectral interferences. Without such correction, the background absorber is indistinguishable from the element being sought and produces calculated values of elemental concentrations which are too high. Background correction systems have been recently reviewed[43]. Most modern AA instrumentation is equipped with optical background correction and there are three types of background correction available commercially.

1) Deuterium Arc System.

This system was introduced in 1965 by Koirtyohann and Pickett[44] and is the most common system in modern instrumentation.

The deuterium arc system has an emission spectrum which is intense up to 400nm but declines to almost zero in the visible wavelength range (see figure 6).

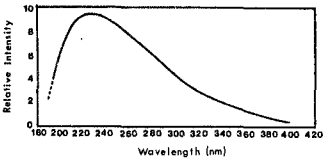

Figure 6 : Spectrum of Deuterium Lamp.

In this system, light from the deuterium arc and the analyte

hollow cathode lamp are alternated rapidly through the sample space. Light from the hollow cathode lamp is absorbed by both the element of analytical interest and the background, whilst light from the deuterium arc is mainly absorbed by the background. The instrument displays the difference between these two as the corrected absorbance.

Deuterium arc systems produce very good background correction for most instances but do have certain limitations. Deuterium background correction cannot correct for structured narrow band spectral interferences, e.g., the measurement of selenium in the presence of iron. There is a degradation of the signal to noise ratio due to the use of two light sources and this method of background correction is not particularly useful in the visible region of the spectrum. There are limitations in the necessity to match the intensities of the source and deuterium lamp and the need to have very good alignment between the optical beams of the source and deuterium lamps. Because of these limitations, other background correction systems have been introduced.

2) Zeeman Background Correction.

Recently the Zeeman effect has been used for background correction in atomic absorption[45] and is particularly useful in electrothermal atomization. In this technique, the spectral light source or the atom cell is placed between the poles of a strong magnet. The spectral line is split into at least three components (see Figure 7). The π component stays at the original wavelength but the σ components, which constitute the background, are shifted away. The π component is polarised in a plane parallel to the magnetic field whilst the σ component is polarized in a perpendicular plane.

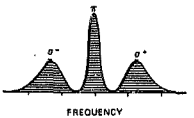

Figure 7 : Normal Zeeman Splitting Pattern.[43]

If the magnets are placed around the atom cell then a rotating polarizer is placed between the light source and the atom cell and the passage of parallel and perpendicular polarized light is alternated. The Zeeman system therfore overcomes many of the weaknesses of the deuterium arc system.

3) Smith Hieftje System.

A new system of background correction has recently been reported[46]. It has been known for some time that if the hollow cathode lamp is pulsed at an excessively high current, the emission lines are broadened and relative atomic absorbance from the analyte is greatly reduced. In the Smith Hieftje system use is made of this phenomenon, called self-reversal. Initially the lamp is run at a low current and its light is absorbed by the analyte element and the background component. Then the lamp is pulsed briefly at a high current, causing self-reversal. As a consequence, absorbance measured during the high current pulse consists principally of that produced by the background component. Subtraction of absorbance values measured during the two pulses then provides a background corrected signal.

1.7.2) Non-spectral Interferences.

1.7.2.1) Condensed Phase Interferences.

This type of interference affects the analyte up to the stage when it is being released from the atomization surface into the gas phase. The furnace processes to be considered here are far more complicated than for spectral interferences and a fundamental knowledge of atom formation processes is required.

1.7.2.1.1) Interference Mechanism.

Analyte can be lost during the ash phase due to volatile compound formation. The most common example of this is loss of analyte by volatilization of volatile halides. This can occur during atomization in hydrochloric acid but is particularily severe for the analysis of sea water.

Incomplete release of the analyte due to the formation of refractory carbide can also account for condensed phase interference. Pyrolytically coated graphite furnaces are reported to give better *sensitivity and less "memory effect"* for the determination of molybdenum and vanadium[47] both of which elements form refractory carbides. However carbide formation is not the only type of interference. The formation of intercallation or lamellar compounds of alkali or alkaline earth metals with graphite may inhibit the release of these elements from the atomizer wall. It has also been suggested that atomization of copper can be inhibited in the presence of alkali or alkaline earth halides by occlusion of the analyte in microcrystals or agglomerates of the matrix material[48].

Interference due to the rate of analyte release is the basic condensed phase interference. This can be caused by changes in the surface of the graphite furnace with time leading to greater porosity and hence reactivity of the surface material. This effect is obviously very difficult to predict and may sometimes be beneficial rather than detrimental.

1.7.2.1.2) Interference Removal.

Removal of the type of interference that is caused by ashing losses is similar to that for spectral interferences. Selective volatilization, classical separation or chemical pretreatment techniques can be used.

For elements forming refractory carbides, the reduction of the graphite surface reactivity by coating with pyrolytic graphite or elimination of carbon from the electrothermal atomizer is desirable to reduce or eliminate carbide formation. The latter may be achieved either by lining the inside of the furnace with a high melting point *metal or by forming a coating of a highly stable carbide.*

The best way to deal with interferences due to time-dependant release and removal of atoms is by the use of a constant temperature furnace. The use of metal atomizers may also reduce interferences due to changes in the graphite furnace although it seems reasonable to expect the surface of the metal atomizer to change also.

Incomplete release of the analyte due to the formation of refractory carbide can also account for condensed phase interference. Pyrolytically coated graphite furnaces are reported to give better sensitivity and less "memory effect" for the determination of molybdenum and vanadium[47] both of which elements form refractory carbides. However carbide formation is not the only type of interference. The formation of intercallation or lamellar compounds of alkali or alkaline earth metals with graphite may inhibit the release of these elements from the atomizer wall. It has also been suggested that atomization of copper can be inhibited in the presence of alkali or alkaline earth halides by occlusion of the analyte in microcrystals or agglomerates of the matrix material[48].

Interference due to the rate of analyte release is the basic condensed phase interference. This can be caused by changes in the surface of the graphite furnace with time leading to greater porosity and hence reactivity of the surface material. This effect is obviously very difficult to predict and may sometimes be beneficial rather than detrimental.

1.7.2.1.2) Interference Removal.

Removal of the type of interference that is caused by ashing losses is similar to that for spectral interferences. Selective volatilization, classical separation or chemical pretreatment techniques can be used.

For elements forming refractory carbides, the reduction of the graphite surface reactivity by coating with pyrolytic graphite or elimination of carbon from the electrothermal atomizer is desirable to reduce or eliminate carbide formation. The latter may be acheived either by lining the inside of the furnace with a high melting point metal or by forming a coating of a highly stable carbide.

The best way to deal with interferences due to time-dependant release and removal of atoms is by the use of a constant temperature furnace. The use of metal atomizers may also reduce interferences due to changes in the graphite furnace although it seems reasonable to expect the surface of the metal atomizer to change also.

1.7.2.2) *Vapour Phase Interferences.*

This type of interference occurs in the gas phase and influences any thermodynamic processes which may be taking place. It has been shown[23] that the vapour inside a pulse heated cylindrical atomizer is in thermal equilibrium provided that the heating rate is less than $10^4 Ks^{-1}$.

1.7.2.2.1) Interference Mechanism.

Unlike flame spectroscopy where dissociation equilibria mainly involve flame components, in electrothermal atomizers the sample matrix is the main source of concomitants entering the dissociation equilibria. Formation of volatile halides is a major cause of vapour phase interference in electrothermal atomization. This type of interference is due to loss of these compounds at temperatures not sufficiently high enough to cause their appreciable dissociation.

Ionization is not a major cause of interference in electrothermal atomization. Recent results of Sturgeon and Berman[49] have confirmed that ionization of lithium, potassium, rubidium and cesium in the graphite furnace at 2300°C is not significant from the viewpoint of atomic absorption but ionization interference should be taken into consideration for potassium, rubidium and cesium when atomic emission is measured.

Interference due to changes in the rate of analyte removal would not be expected to be as important as changes in the rate of analyte supply since in pulsed-type atomizers the removal function is sufficiently rapid relative to the supply function.

1.7.2.2.2) Interference Removal.

Similar to spectral interferences, the major cause of vapour phase interferences is the formation of gaseous monohalides. As a consequence interference removal will also involve classical separations, selective volatilization, chemical pretreatment, electrodeposition and the use of a L'vov type platform. (As dicussed in 1.7.1.2)

An investigation was therefore undertaken to determine the feasibility of measuring some or all of the lanthanoids by electrothermal atomization and to try to determine atomization mechanisms and possible interelement interference effects.

CHAPTER 2

SELECTION OF OPERATING CONDITIONS

2.1) DETERMINATION OF THE LANTHANOIDS BY ELECTROTHERMAL ATOMIZATION.

Electrothermal atomization has been used in the measurement of *individual or selected* groups of the lanthanoids. Fuavao and Sneddon[50] measured ytterbium and compared atomization from furnace wall, [illegible]form and a microboat. Grobenski[51] measured all the lanthanoids using both unpyrolytically and pyrolytically coated graphite furnaces and *posulated a possible atomization mechanism.* Sen Gupta determined the lanthanoids and yttrium in rocks[52] and in sixteen international reference materials of *rock and coal*[53]. Horsky and Fletcher[54] used a combined ion exchange/graphite furnace procedure to determine five of the lanthanoids *in geological* samples. L'vov and Pelieva[55] lined the graphite furnace with tantalum foil and found that the sensitivity for all the lanthanoids tested was improved. Menzucotelli et al investigated the determination of dysprosium, europium, thullium, holmium and ytterbium by graphite furnace AAS[56] and interference effects on the determination of ytterbium, holmium, dysprosium, thullium[57] and europium[58].

The aims of this investigation were to determine the applicability of electrothermal atomization for the determination of the lanthanoids and to determine optimum conditions of measurement, *to investigate* atomization processes and interference effects and to develop an analytical method for the measurement of individual *lanthanoids in a mixed lanthanoid matrix.*

2.2) EQUIPMENT USED.

In this study a Varian *AA1275 single beam atomic absorption* spectrophotometer was used in conjunction with a Varian GTA-95 electrothermal atomizer. The system is equipped with an *autosampler* for injection of predetermined sample volumes to the graphite

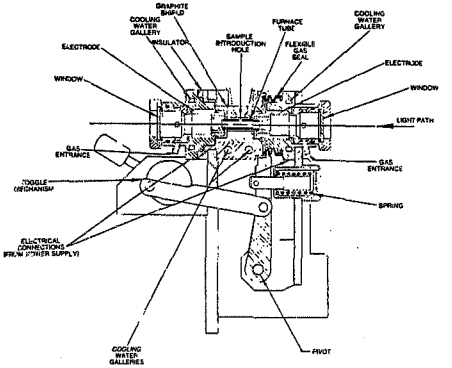

Figure 5 ; Cross Section of the Varian GTA-95 Furnace System[59].

furnace.

A cross section of the furnace is shown in Figure 8. Electrical contact to the furnace is acheived by the use of water cooled chamfered graphite collars which are spring loaded to ensure constant contact and therefore reproducible temperatures. Voltage feedback control is used to control temperature settings as there is no thermocouple or optical pyrometer in the system. Voltage and temperature settings are calibrated by the manufacturer.

During the dry, ash and atomize cycle, inert gas can be passed around the outside as well as through the the inside of the furnace, in the latter case exiting through the sample introduction hole. For maximum sensitivity no gas should flow through the centre of the furnace during atomization, however the GTA-95 system allows the flow rate to be varied between 0 and 3 litres per minute. Increasing the flow rate of gas decreases the analyte signal since the gas flowing through the furnace effectively "sweeps out" the analyte atoms and hence the reduces the residence time in the light path which reduces the sensitivity.

The programming facility on the GTA-95 consists of a menu driven system consisting of "three pages" of suitable operating parameters which are displayed on the visual display unit. The first page contains furnace conditions and has up to twenty programmable steps. Temperature, time, gas flow rate, gas type and read command can all be programmed (Figure 9) There are two inlets for the sheath gas labelled NORMAL and ALTERNATE. Therefore two types of sheath gas can be permanently connected to the instrument. In this study argon was connected to the inlet labelled NORMAL. The read command when switched on (i.e. marked * in the read command column) is a trigger to the spectrophotometer to read the integrated absorbance signal (either peak height or peak area), this is usually over the entire atomization cycle. There is no automatic ramp rate selection therefore the rate of increase in temperature has to programmed in as a separate step. In the example shown in Fig.8, steps 1 to 3 are the dry phase, steps 4 to 6 are the ash phase, steps 7 to 8 are the atomize phase and steps 9 to 10 are the tube clean phase.

The second page is a graphics display of page one (i.e. temperature/time profile). This page is automatically displayed

FURNACE OPERATING PARAMETERS.

STEP NO.	TEMPERATURE °C.	TIME SEC.	GAS FLOW	GAS TYPE	READ COMMAND	
1	75	5.0	3.0	NORMAL		
2	95	30	3.0	NORMAL		
3	95	30	3.0	NORMAL		
4	1000	10	3.0	NORMAL		
5	1000	10	3.0	NORMAL		
6	1000	2.0	.0	NORMAL		
7	2700	.9	.0	NORMAL	*	
8	2700	5.0	.0	NORMAL	*	
9	2800	.1	3.0	NORMAL		
10	2800	3.0	3.0	NORMAL		

Figure 9 : Example of Furnace Program Parameters.

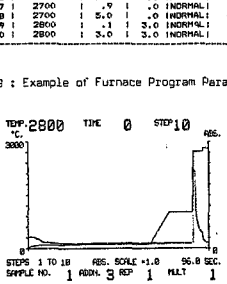

Figure 10 : Example of Temperature/Time, Absorbance/Time Profile.

SAMPLER PARAMETERS NORMAL CALIBRATION

SAMPLES AND STANDARDS TYPE	LOCATION	VOLUME	BLANK VOLUME	MODIFIER VOLUME
BLANK	--	--	25	
STD 1	51	5	20	
STD 2	51	10	15	
STD 3	51	15	10	
STD 4	51	20	5	
STD 5	51	25		
SAMPLES	--	25		

LAST SAMPLE NO.	= 4	MULTIPLE INJECTIONS	= 1
NO. OF REPLICATES	= 2	LAST DRY PHASE STEP	= 2
RESLOPE RATE	=	INJECTION TEMP.	=AMB
FIRST SAMPLE NO.	= 3		

Figure 11 : Example of Autosampler Conditions.

while the furnace is operating and the analytical signal is superimposed on the temperature/time profile. A hard copy of this can be obtained if a printer is incorporated in the system. An example of this output is shown in Figure 10.

The third page is devoted to autosampler conditions. Autosample, single sample and standard additions can be used. Varying volumes up to 70µl can be transferred to the furnace and there is also a facility for adding chemical modifiers to samples and standards. Multiple injections can be made and the injection temperature can be varied from 40 to 150°C in which case the furnace maintains a preset temperature during sample injection or the injection temperature can be set to ambient in which case the furnace cools to room temperature. An example is shown in Figure 11.

2.3) INSTRUMENT CONDITIONS.

The resonance wavelengths and lamp currents used are detailed in Table 4. A spectral bandwidth of 0.2 nm was used for the determination of all the lanthanoids in order to reduce the contribution of incandescence. For the same reason, the alignment of the graphite furnace in the light path was optimized.

2.4) ESTABLISHMENT OF OPERATING CONDITIONS.

Operating conditions were established for twelve of the lanthanoids (viz. Dysprosium, erbium, europium, gadolinium, holmium, neodynium, praseodynium, samarium, terbium, thullium, ytterbium and lutetium) in two sets of synthetic standard solutions, one containing 1 per cent v/v hydrochloric acid and one containing 1 per cent v/v nitric acid.

The results were as follows :

i) Dry Stage. A dentist's mirror was used to observe the sample drying in the furnace. A temperature of 95°C allowed uniform drying with no sputtering. The drying time was dependent on the volume of solution injected into the furnace. A time of 55 seconds was necessary to dry 25 µl.

ii) Ash Stage. To determine the ash temperature the atomization

Table 4 : Wavelengths and Lamp Currents used for the Measurement of the Lanthanoids.

Lanthanoid	Lamp Current (mA)	Wavelength (nm)
Praseodynium	15	495.14
Neodynium	15	463.42
Samarium	8	429.67
Europium	8	459.40
Gadolinium	10	407.87
Terbium	10	432.65
Dysprosium	10	421.17
Holmium	10	410.38
Erbium	10	400.80
Thullium	10	371.79
Ytterbium	15	398.80
Lutetium	10	335.96

temperature was set to 2800°C and the dry temperature to optimum. The ash temperature was then varied and the atomization peak height recorded. A decrease in atomization peak height is usually an indication of loss of analyte due to volatilization. In the case of the lanthanoids, an increase in ash temperature, at temperatures well below the volatilization temperature of these elements, caused a decrease in peak height. This reduction was not caused by analyte loss but probably by the formation of refractory compounds. This phenomenum is usually associated with carbide forming elements since elevated temperatures allow greater probability of carbide formation. Therefore in most instances the ash temperature chosen was not necessarily the temperature which gave maximum sensitivity but was that temperature for which the sensitivity loss was not due to analyte volatilization. An example of a typical ash temperature curve is shown in Fig. 12. The ash time for the simple hydrochloric or nitric acid matrix was 10 seconds. The ash temperatures used for the measurement of the twelve elements investigated are shown in Table 5.

iii) Atomization Stage. To determine the optimum atomization temperature, the dry and ash temperatures were maintained at the optimum values established in the previous sections and the atomization temperature varied. It was found that increasing atomization temperatures caused increasing peak heights as would be expected. However the lanthanoids are known to form refractory compounds in the furnace and the effect of increasing atomization temperature on the blank peak (i.e. an atomization of acid only, after an analyte atomization) was also tested. Photo emission from the furnace walls at high temperatures severely affected measurements of some of the lanthanoids (Figure 13) while lower atomization temperatures resulted in incomplete analyte volatilization giving rise to "memory effects". Therefore the atomization temperatures used were those which gave reasonable sensitivity for the analyte but for which the "memory effect" was not severe. Atomization temperature was maintained for five seconds since longer times did not effectively reduce the blank and only served to reduce the useable life of the graphite furnace. From this work, optimum atomization temperatures were established and are detailed in Table 5.

In all cases, there was no difference in conditions between

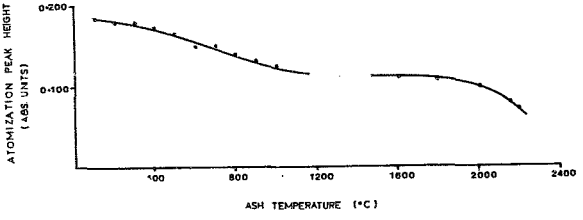

Figure 12 : Typical Volatilization Curve for the Lanthanoids.

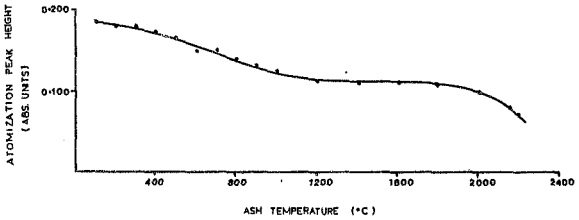

Figure 12 : Typical Volatilization Curve for the Lanthanoids.

Table 5 : Optimized conditions for the measurement of the lanthanoids in synthetic solutions.

Lanthanoid	Ash Temp. °C	Optimum Atomization Temp. °C
Praseodynium	700	2600
Neodynium	900	2800
Samarium	800	2800
Europium	700	2700
Gadolinium	900	2700
Terbium	600	2500
Dysprosium	700	2800
Holmium	700	2600
Erbium	800	2800
Thullium	700	2800
Ytterbium	900	2700
Lutetium	800	2800

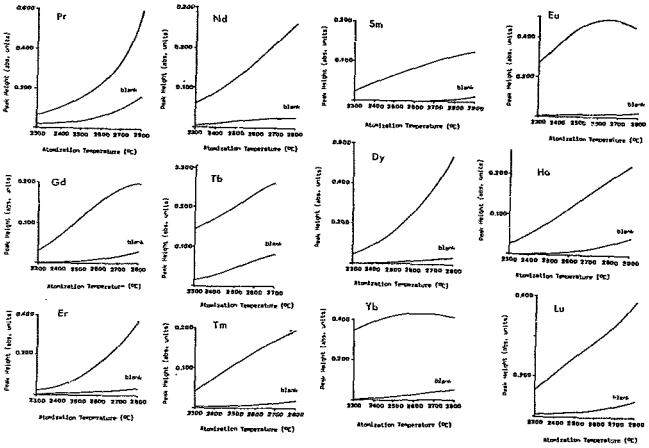

Figure 13 : Effect of Atomization Temperature on the Blank Peak for the Lanthanoids.

synthetic solutions in either hydrochloric or nitric acid.

2.5) SENSITIVITY AND PRECISION OF MEASUREMENT.

Calibration curves were obtained for each of the lanthanoids in both hydrochloric and nitric acids (1%v/v). Results obtained in both hydrochloric and nitric acids for thullium, ytterbium and europium were comparable. However for the other lanthanoids the sensitivity, at higher concentrations of analyte, was better in hydrochloric acid rather than nitric acid. This may be due to refractory compound formation in the nitric acid matrix which inhibits volatilization of the lanthanoid from the graphite surface.

From this work, the quantity of each lanthanoid required to give an atomization peak height of 0.100 absorbance units (minus the blank absorbance) was calculated. The values obtained for each of the lanthanoids were compared, relative sensitivies calculated, plotted and compared with the boiling points of the lanthanoid metals and their heats of sublimation (Figure 14). These plots are in agreement with Grobensky's results[48] and suggest that a change in electronic structure is related to the boiling and sublimation ranges of the various lanthanoids and is directly linked to the number of free atoms present i.e. the sensitivity.

An indication of the relative variation in optimum precision for each element was established in synthetic solutions of each element (Table 6). For most elements relative standard deviations (s_r) for solutions containing nitric acid were slightly inferior to those containing hydrochloric acid which is probably due to the increased quantity of oxygen in the system in the nitric acid matrix.

It was then decided to investigate atomization processes and interference effects on only three of the lanthanoid elements. Europium was chosen because its measurement by electrothermal atomization was relatively uncomplicated and it was one of the more sensitive elements. Terbium was chosen because its measurement by electrothermal atomization was quite complicated and its sensitivity was poor. Finally samarium was chosen because its sensitivity and ease of measurement was somewhere between that of europium and terbium.

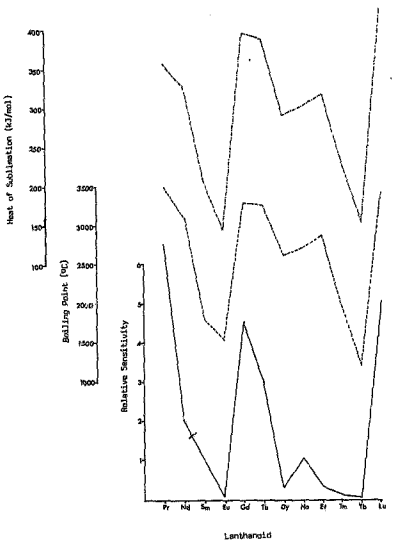

Figure 14 : Relative Sensitivities, Heats of Sublimation and Boiling Points for the Lanthanoids.

Table 8 : Precision of Measurement for the Lanthanoids in Synthetic Solutions.

Lanthanoid	Acid Medium (1% v/v)	s_r
Praseodynium	HCl	0.065
	HNO_3	0.130
Neodynium	HCl	0.044
	HNO_3	0.078
Samarium	HCl	0.024
	HNO_3	0.056
Europium	HCl	0.028
	HNO_3	0.028
Gadolinium	HCl	0.095
	HNO_3	0.150
Terbium	HCl	0.045
	HNO_3	0.082
Dysprosium	HCl	0.041
	HNO_3	0.061
Holmium	HCl	0.021
	HNO_3	0.045
Erbium	HCl	0.020
	HNO_3	0.060
Thullium	HCl	0.031
	HNO_3	0.041
Ytterbium	HCl	0.022
	HNO_3	0.024
Lutetium	HCl	0.045
	HNO_3	0.056

CHAPTER 3

SAMARIUM, TERBIUM AND EUROPIUM.

3.1) INTRODUCTION.

Samarium, terbium and europium were investigated in order to determine the atomization processes in the furnace. Appearance temperatures and atomization profiles from graphite and tantalum were determined and compared for each of the analytes. Arrhenius type investigations were carried out to determine the atomization processes for the analytes. Finally an attempt was made to identify the products present in the furnace prior to atomization by the use of X-ray diffraction techniques and to determine the efficiency of atomization by measuring the amount of residual analyte in the furnace after atomization by instrumental neutron activation analysis.

3.2) APPEARANCE TEMPERATURES.

The appearance temperature was determined experimentally by the method of Campbell and Ottoway[80] and compared to the theoretical.

In a hydrochloric acid matrix, the chloride complex is usually present prior to atomization, however in a nitric acid matrix the nitrates usually thermally dissociate to the oxides. However the lanthanoid chlorides all hydrolyse to the oxychlorides on evaporation and above 1000°C these decompose to the oxide. Therefore in the case of the lanthanoids, the oxide intermediate prior to atomization can be expected in both acid media.

$$M_2O_3(s) + 3C(s) \rightarrow 3CO(g) + 2M(g)$$

The overall free energy of this reaction is given by the sum of the free energies of the products minus the sum of the free energies of the reactants.

$$\Delta G_{react} = 3x\ \Delta G_f\ CO(g) + 2x\ \Delta G_f\ M(g) - \Delta G_f\ M_2O_3(s) - 3x\ \Delta G_f\ C(s)$$

For the above reaction to be thermodynamically feasible, the free energy of the reaction must be negative. If the free energies of the individual components are known then the free energy of reaction can be calculated.

The appearance temperatures, for the three lanthanoids, were determined experimentally as follows. Using a constant dry and ash temperatures, the atomization temperature was varied in order to determine the appearance temperature. A quantity of analyte was atomized to give full scale deflection at the optimum atomization temperature for that analyte. The atomization temperature was then reduced to no analyte signal then increased in 20 degree increments until about 3 to 5 percent of full scale deflection was obtained. A tube clean phase was incorporated to remove any residual analyte.

The results are tabulated below, the analyte boiling points are included for comparison.

Table 7 : Comparison of theoretical and experimental appearance temperatures for three lanthanoids.

Element	Melting Point °C	Boiling Point °C	Temperature for negative ΔG °C	Appearance Temperature °C
Europium	822	1529	2027	1760-1840
Samarium	1074	1794	2377	1900-1950
Terbium	1365	3230	2727	2150-2200

It is important to note that all the elements appearance temperatures are above the boiling point of the metal suggesting that $M(s) \rightarrow M(g)$ is not a contributary process. The fact that the appearance temperature is lower than predicted suggests that carbothermal reduction of the oxide is also not a contributary

process.

Several authors have criticised this approach. Sturgeon et al[31] claim that the appearance temperature should be determined at the beginning of the analyte signal and that measurement of the analytical peak at a predetermined temperature, as in the Campbell and Ottoway method, will result in an appearance temperature which is too high. Fuller[31] states that thermodynamics alone cannot be used to determine atomization processes and that kinetics must be used to determine the reaction rates for the atomization processes.

3.3) ATOMIZATION PROFILES.

The atomization peak shape obtained for an element is indicative of the type of processes by which the element volatilizes from the graphite furnace. Ideally a Gaussian peak should be obtained but this is rarely the case. A double atomization peak can be indicative of two atomization processes or of matrix interference. An atomization peak which rises to a maximum but falls slowly to the baseline with a lot of tailing can be indicative of refractory compound formation. It is also very useful to compare atomization peaks from different types of surface e.g. a graphite surface with a metal surface. The atomization profiles for the three lanthanoids were investigated.

Using the page two facility of the GTA-95 it is possible to obtain a printed copy of the absorbance/time curves and hence the atomization profiles.

Absorbance/time curves were obtained for samarium, europium and terbium, using the optimum conditions established, from a graphite surface. As a comparison, these elements were also atomized from a tantalum surface.

A tantalum insert was made from pure tantalum foil of thickness 0.062 mm. These inserts were shaped to fit closely inside a graphite surface and the analyte was injected onto and atomized from this surface. Operating conditions had to be changed since the melting point of tantalum is 2996°C. A maximum atomization temperature of 2500°C was used since higher temperatures damaged the tantalum surface causing it to become very brittle. The dry temperature was

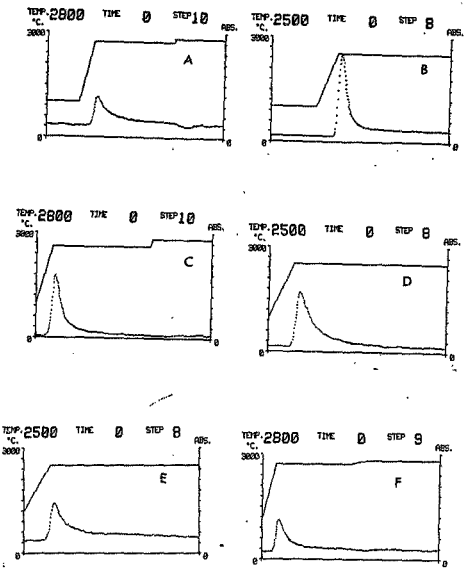

Figure 15 : Atomization Profiles of (A) Terbium from a Graphite Surface, (B) Terbium from a Tantalum Surface, (C) Samarium from a Graphite Surface, (D) Samarium from a Tantalum Surface, (E) Europium from a Graphite Surface and (F) Europium from a Tantalum Surface.

increased to facilitate more uniform drying.

Comparison of the two atomization profiles for each of the analytes is shown in Figure 15. The atomization profiles for samarium and europium from both tantalum and graphite are comparable suggesting a similar atomization process in each case. However in the case of terbium, atomization from graphite produces a profile in which the peak is not very sharp and there is a lot of tailing at the end of the atomization cycle (see Figure 15A). Atomization from tantalum produces a peak in which the terbium appears to atomize much faster and there is very little tailing (see Figure 15B). This suggests that atomization from graphite and tantalum occur by two different processes. In the case of graphite, terbium forms a highly refractory compound which is not completely atomized. This may be carbide formation since it is not present during atomization from tantalum.

The tantalum insert was found to be impractical since after only one atomization the tantalum began to curl at the edges reducing the contact surface and causing arcing and hence irregular heating of the tantalum. After only five atomizations the tantalum became very brittle and could not be used. It was decided to use a longer piece of tantalum foil. The foil used this time was 0.018 mm thick and was cut and shaped to fit inside the furnace and to extend out of each end of the furnace. When the graphite furnace was placed into the furnace assembly system, the tantalum was then in contact with the graphite collars which would facilitate more regular heating of the tantalum. Results from this type of tantalum surface were similar to those of the other tantalum insert but more reproducible. However the lifetime of the strip was not improved.

An attempt was made to produce a tantalum insert from pure tantalum rod. This type of insert was made in the shape of a boat which fitted inside the furnace and made good contact with the furnace walls. A diagram the boat is shown in Figure 16.

Figure 16 : Diagram of a Tantalum Boat.

The tantalum boat was tested with respect to *terbium* since atomization of samarium or europium from a *tantalum* surface does not improve the peak. Due to the shape of this boat a maximum volume of 10 µl could be pipetted onto it without spillage. A maximum atomization temperature of 2300°C was used since higher temperatures caused the tantalum to "smoke" (i.e. fragmentation particles, generated from the tantalum, in the light path) which interfered with the terbium measurement and probably reduced the useable lifetime of the boat. Again the atomization peak was improved. However there appears to be a temperature lag between furnace and boat temperature since the atomization peak is shifted to the right in the temperature/time, absorbance/time profile. Ten atomizations of 10 µl of 10 µg/ml terbium were made from which a relative standard deviation of 30 per cent was obtained. The positioning of the boat inside the furnace appears to be critical since its removal and replacement caused a deterioration in peak shape. After approximately sixty atomizations, the atomization peaks became irregular in shape (i.e. noisy peaks with lots of spikes) although the tantalum boat did not appear to have deteriorated.

Further tests were then carried out using a tantalum platform. This was made from pure tantalum rod to the same design of the commercially available graphite platforms (see Figure 17).

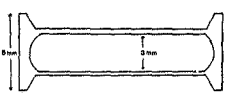

Figure 17 : Diagram of a Tantalum Platform.

Since contact with the furnace wall only occurs at two points heating of the platform will be mainly due to convection and the temperature of the platform will lag that of the wall. This platform was tested for terbium. Atomization temperatures above 2300°C caused the signal to be overrange even when there was no terbium on the platform. This effect is probably due to either tantalum being released in the light path or the fact that the tantalum platform vibrates which may also interfere with the light path. However at 2300°C, the terbium is not totally released from the platform and the atomization peaks obtained are broadened with a lot of tailing. Therefore sensitivity is poor and this platform is not suitable for the measurement of terbium.

An attempt was made to form a tantalum carbide coating on an unpyrolytically coated graphite furnace. The method of Fritzsche et al[21] was used in which the graphite furnace is soaked overnight in a solution of 5 per cent tantalum in hydrofluoric acid. The furnace is then dried at 120°C for 2 to 4 hours. Prior to atomization the furnace is heated to 120°C for 1 minute, then to 400°C for 30 seconds and finally to 2200°C within 90 seconds and held at maximum temperature for 10 seconds. This procedure was repeated twice. This furnace was tested for terbium but showed no improvement in atomization peak. In fact the peak obtained from the carbide coated furnace was worse than the atomization peak from a pyrolytically coated furnace. Atomization of terbium from an unpyrolytically coated graphite furnace resulted in a peak which was similar to the peak obtained from the carbide coated surface. Sensitivity was poor and the atomization peak was broadened with a lot of tailing. It was thought that soaking the furnaces in the tantalum solution under vacuum would improve the carbide coating. However when this was tried there was no improvement in results. This type of carbide coating does not appear to offer any improvement in results. This could be due to some sort of chemical reaction between terbium and tantalum carbide but it is more likely that the coating was not satisfactory.

3.4) ARRHENIUS TYPE INVESTIGATIONS.

The use of either thermodynamic or kinetic principles to understand atomization processes can be an oversimplification. The graphite furnace, during atomization, contains a highly dynamic environment and if thermal equilibrium exists it will be very transient. The model proposed by Fuller[31] using kinetics has disadvantages since in normal graphite furnace analyses accurate vapour temperatures are not known. The model of Torsi and Tessari[30] is only applicable to open type atomizers. With normal graphite furnaces recondensation has been shown to occur (see Chapter 3 section 3.5)

Therefore it was decided to investigate the model of Sturgeon et al[61] in which both the kinetic and thermodynamic aspects of atomization are taken into account.

3.4.1) Theory.

As discused previously (Chapter 1, Section 1.6.8.) there are several atomization processes which can occur in the graphite furnace.

$$M_xO_y(s/l) \rightarrow M_xO_y(g) \rightarrow xM(g) + yO(g) \quad \text{.....(1)}$$

$$M_xO_y(s/l) + yC(s) \rightarrow xM(s/l) + yCO(g)$$

$$x/2\ M_2 \rightarrow xM(g) \quad \text{.....(2)}$$

$$MX_m(s/l) \rightarrow MX_m(g) \rightarrow M(g) + X(g) \quad \text{.....(3)}$$

The oxygen and halogen have been shown in monatomic form since the partial pressures of these species, in the gas phase, are very small. Very small masses of sample are atomized in the furnace and therefore the partial pressures of any liberated oxygen or halogen within the furnace is also very small. Therefore the possibility of recombination through collision of analyte fragments is insignificant.

In the general atomization processes (1) to (3), if the final step is characterized by a unimolecular rate constant k_1, then for reaction (1) the rate of production of $M(g)$ at any temperature is given by :

$$dP_{M(g)}/dt = xk_1P_{M_xO_y(g)}$$
$$= k_1K_pa_sx \qquad \text{.....(4)}$$

Where $K_p = P_{M_xO_y(g)}/a_s$

a_s = activity of the condensed phase on the surface of the carbon surface.

P = partial pressure of species denoted by the subscript of P.

The activity of the surface phase will be maintained as a variable in this model since it is dependant on both analyte mass and temperature.

There is also a possibility of loss of atomic vapour by diffusive and convective processes. Therefore it is necessary to introduce a term R_D into equation (4) to account for these losses.

$$dP_{M(g)}/dt = k_1K_pa_sx - R_D \qquad \text{.....(5)}$$

The distribution of atomic vapour along the length of the furnace is roughly Gaussian and is governed by Fick's second law. Assuming that the vapour density falls linearly from its maximum in the centre to zero where the vapour leaves the furnace by condensation at either end, then the rate of diffusional loss from the furnace may be approximated by a simple first order process.

$$R_D = k_DP_{M(g)}$$

where k_D is the rate constant for loss of vapour.

For a short period of time, the activity (a_s) is nearly constant and a steady state is acheived, under these conditions equation (5) can be written thus :

$$dP_{M(g)}/dt = 0 = k_1 K_p a_s x - k_D P_{M(g)} \quad \ldots\ldots\ldots\ldots (6)$$

which on rearrangement yields :

$$P_{M(g)} = k_1 K_p a_s x / k_D \quad \ldots\ldots\ldots\ldots (7)$$

In atomic absorption spectroscopy the measured absorbance A is directly proportional to the concentration. Therefore :

$$A_T = k_A P_{M(g)} = k_A k_1 K_p a_s x / k_D \quad \ldots\ldots\ldots\ldots (8)$$

where A_T is the absorbance of a metal vapour at temperature T and k_A is the proportionality constant.

According to transition state theory the rate constant k_1 can be formulated in thermodynamic terms by the introduction of the standard free energy change for the reaction.

$$k_1 = kT/h \exp(-\Delta G^\circ_r/RT)$$
$$= (kT/h)\exp(-\Delta S^\circ_r/R)\exp(-\Delta H^\circ_r/RT) \quad \ldots\ldots\ldots\ldots (9)$$

where k is Boltzmann's constant, h is Planck's constant and ΔG°_r, ΔS°_r and ΔH°_r are the free energy, entropy and enthalpy of activation respectively. It is possible to equate the enthalpy of activation to the activation energy to a first approximation. The equilibrium constant for the gas-condensed phase equilibrium (K_p) is a function of temperature and its relationship is given by the van't Hoff equation.

$$\left(\frac{\partial \ln K_p}{\partial (1/T)_p}\right)_p = \frac{-\Delta H^\circ}{R} \quad \ldots\ldots\ldots\ldots (10)$$

where ΔH° is the standard enthalpy change for a phase transition and R is the gas constant.

On integration, using common logarithms equation (9) becomes :

$$\ln K_p = -\Delta H^o/2.3RT + C \qquad \ldots\ldots\ldots\ldots(11)$$

where C is the integration constant. ΔH^o is assumed to be temperature independant since the product $\Delta T \Delta C_p$ is small compared to ΔH^o.

Substituting equations (9) and (11) in (8) gives :

$$\ln A_T = \frac{-E_a + \Delta H^o}{2.3RT} + \frac{\Delta S^o_r}{2.3R} + \frac{k_A a_s k T x C'}{h k_D}$$

$$= \frac{-E_a + \Delta H^o}{2.3RT} + A_o$$

If the log of the absorbance is plotted against the inverse of the absolute temperature then a straight line with slope of $-(E_a - \Delta H^o)2.3R$ and intercept A_o should be obtained.

The activation energy obtained from lnA versus 1/T plot is an excellent approximation to the bond dissociation energies of gaseous species and can be best correlated to one of the following values :

1) The dissociation energy of the metal oxide. i.e. free atoms arise from thermal dissociation of the oxide.
2) The dissociation energy of the metal halide.
3) The heat of atomization of the metal. i.e. carbothermal reduction of the metal oxide yielding solid or liquid metal which volatilizes to gaseous metal.
4) The metal-metal bond dissociation energy. i.e. formation of dimeric species with atomization sequence as above.
5) The metal-carbon bond dissociation energy. i.e. formation of carbides prior to atomization.

It is possible that atomization may occur by a different process at different temperatures. Take for example equation (1)

$$M_xO_y(s/l) \xrightarrow{(1)} M_xO_y(g) \xrightarrow{(2)} xM(g) + yO(g)$$

At low temperatures when little of the oxide has vapourized then reaction (1) may be expected to be the major supplier of M(g). At higher temperatures reaction (2) may be the more likely process.

Therefore the E_a plots obtained may be a composite of two straight lines with different slopes.

3.4.2) *Experimental.*

The E_a plots for europium, samarium and terbium were determined using the method of Sastry et al[62]. The analyte is atomized from the graphite furnace at a preset temperature, the peak height obtained is taken as the absorbance and the temperature displayed by the instrument is taken as the atomization temperature. They claim that this is possible because during atomization of compounds of low volatility ... there will not be much difference between gas and wall temperatures. In the GTA-95 system used for this study, the furnace temperature is controlled by voltage feedback which should compensate for any change in resistance and therefore the temperature programmed should be the temperature attained by the furnace.

Measurements were made in synthetic solutions of the appropriate analyte in 1 per cent hydrochloric acid. Argon was used as the sheath gas and the flow of gas was stopped during atomization. The peak heights were recorded in absorbance units at varying atomization temperatures from around 2000°C to 2900°C in one hundred degree stages.

Results for each of the analytes are detailed below.

a) Europium

Two straight lines were obtained which intersected at approximately 2350°C (see Figure 18a). The activation energy at the higher temperature region was 163 kJ/mol which is comparable to 144.7 kJ/mol, the heat of sublimation of europium. The activation energy at the low temperature region was 259 kJ/mol. The heat of dissociation of europium monoxide is 479 kJ/mol[63] which is not comparable to the activation energy for the low temperature region. However the heat of dissociation of europium dicarbide is 215 kJ/mol[64] which is comparable to the activation energy. This suggests that thermal dissociation of the dicarbide is the most likely process at low temperatures and at high temperatures

Eu(s) → Eu(g) is the more likely process. The boiling point of europium metal is 1529°C so it is possible that europium is in the gaseous state above 2350°C.

b) Samarium

Two straight lines were obtained which intersect at approximately 2400°C (see Figure 18b). The activation energy at the higher temperature region was 201 kJ/mol which is comparable to 206.7 kJ/mol, the heat of sublimation of samarium metal. The boiling point of samarium is 1794°C so samarium in the gaseous state is feasible at this temperature. The activation energy at the low temperature region was 410 kJ/mol. The dissociation energy of samarium monoxide is 567 kJ/mol[63] and the dissociation energy of samarium dicarbide is 373.1 kJ/mol[65] neither of which are comparable with the activation energy.

c) Terbium

Two staight lines which intersect at approximately 2300°C (see Figure 18c). The activation energy at the higher temperature region is 155 kJ/mol. This does not compare well with the heat of sublimation for terbium which is 388.7 kJ/mol. The boiling point of terbium is 3230°C suggesting that terbium in the gaseous state is unlikely at these temperatures. The activation energy at the low temperature region is 520 kJ/mol. This value is not comparable to either the bond dissociation energy of terbium monoxide[63] (704 kJ/mol) or terbium dicarbide[66] (628 kJ/mol).

A summary of the results obtained for the three lanthanoids is given in Table 8.

It is possible that these results are questionable especially at the lower temperatures where atomization may not be complete and the rate of atomization may differ and hence affect the peak height.

Sturgeon et al[61] suggested that the absorbance and temperature were measured during the rise of the analytical peak. They used a thermocouple to determine temperature and a storage oscilloscope to collect the peak. However in this investigation this could not be carried out because measurement of the furnace temperature in the GTA-95 system was impossible using the equipment available.

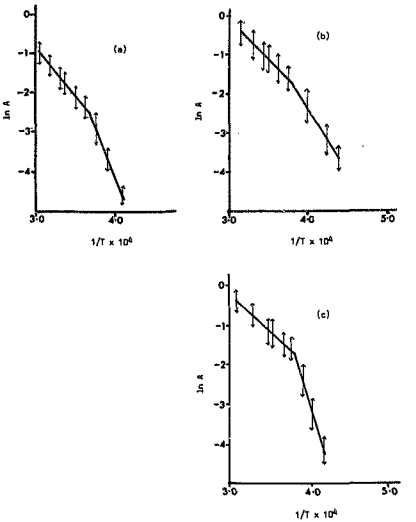

Figure 18 : (a) Plot of ln A vs 1/T for Europium.
(b) Plot of ln A vs 1/T for Samarium.
(c) Plot of ln A vs 1/T for Terbium.

Table 8 : Summary of Activation Energies and Possible Atomization Mechanisms for Europium, Samarium and Terbium.

Element	E_a kJ/mol	Likely intermediate	Energy (kJ/mol)
Europium	259	EuC_2/Eu	218
	163	$Eu(s)/Eu(g)$	144.7
Samarium	410	No correlation	
	201	$Sm(s)/Sm(g)$	206.7
Terbium	520	No correlation	
	155	No correlation	

3.5) NEUTRON ACTIVATION ANALYSIS RESULTS.

The lanthanoids would be ...o form refractory compounds in the furnace. These compounds ...t be completely atomized from the furnace and therefore it was decided to carry out experiments to determine how much residual analyte was left in the furnace after atomization.

A set of furnaces were supplied to the National Physics Research Unit (NPRU) of the University of the Witwatersrand for analysis. These consisted of a blank furnace and for each of terbium, samarium and europium, one furnace with a known quantity of analyte dried onto it and one furnace with the same amount of analyte atomized. Therefore some measure of the efficiency of atomization could be made.

Synthetic solutions of each lanthanoid in one per cent hydrochloric acid were used in each case. Optimum furnace conditions were used but no tube clean stage was included.

Each furnace tube was sealed in quartz and irradiated in the reactor at Pelindaba for at least 14 hours. The samples were allowed to decay for a certain length of time before measurement. Samarium

was measured first since it has the shortest decay period. Terbium and europium have similar decay periods.

Measurement of the furnaces was carried out at NPRU using the equipment available. The system used consisted of a coaxial germanium(lithium) detector coupled to a multichannel analyser. The digital output was recorded on magnetic tape and eventually processed by the computer.

3.5.1) Results for Samarium.

The results obtained are tabulated in Table 9. Precision of measurement was approximately one per cent. Furnace number 1 is the blank furnace, furnace number 2 contained 50 ng of samarium and furnace number 3 is the one from which 50 ng of samarium had been added and then atomized.

Table 9 : Results of Neutron Activation Analysis for Samarium.

Furnace Number	Samarium Counts
1	$(3.80 \pm 0.76) \times 10^3$
2	$(7.54 \pm 0.02) \times 10^5$
3	$(3.85 \pm 0.02) \times 10^5$

From these results, it appears that only 50 per cent of the samarium on the furnace is atomized. However a temperature gradient along the furnace length may cause recondensation at the furnace ends. Each furnace, except the blank, was cut into three portions and the centre of the furnace counted separately from both ends which were counted together. These results (shown in Table 10) indicate that 82 per cent of the samarium is atomized from the centre of the furnace leaving 18 per cent residual. However 31 per cent of the samarium had recondensed on the furnace ends.

Table 10 . Neutron Activation Analysis of Portions of Graphite Furnace for Samarium.

Furnace Number	Samarium Counts
2 (centre portion)	$(5.46 \pm 0.03) \times 10^5$
2 (end portions)	$(2.80 \pm 0.34) \times 10^3$
3 (centre portion)	$(9.78 \pm 0.10) \times 10^4$
3 (end portions)	$(1.73 \pm 0.02) \times 10^5$

3.5.2) Results for Terbium.

Results were obtained similarly for terbium. In this case 500 ng of terbium was dried onto furnace number 4 and atomized from furnace number 5. Precision of measurement was around 3 per cent. Results from the analysis of the entire furnace indicated that only 41 per cent of the terbium had been atomized. These furnaces were also cut into three portions and the centre portion measured separately from both ends which were measured together. Examination of these results (see Table 11) shows that approximately 60 per cent of the terbium had been atomized leaving a residual 40 per cent on the furnace.

Table 11 : Neutron Activation Analysis of Portioned Graphite Furnaces for Terbium.

Furnace Number	Terbium Counts
4 (centre portion)	$(2.56 \pm 0.08) \times 10^8$
4 (end portions)	$(1.98 \pm 0.78) \times 10^6$
5 (centre portion)	$(1.46 \pm 0.06) \times 10^8$
5 (end portions)	$(2.51 \pm 0.28) \times 10^6$

In this case, precision of measurement for the end portions of furnace 4 and 5 was around 20 per cent because the quantity of terbium was reduced. Precision of measurement for the centre portion

was 2 per cent.

3.5.3) Results for Europium.

These were again obtained similarly to both samarium and terbium. In this case 5 ng of europium was dried onto furnace number 6 and atomized from furnace number 7. Results for the analysis of the entire furnace indicated that only 38 percent of the europium had been atomized from the furnace. Again the furnace was cut into three portions and the amount of europium present in the centre portion determined separately from the end portions. These results are presented in Table 12. These results indicate that aproximately 80 per cent of the europium has been atomized.

Table 12 : Neutron Activation Analysis Results of the Portioned Graphite Furnace for Europium.

Furnace Number	Europium counts
6 (centre portion)	$(2.78 \pm 0.14) \times 10^2$
6 (end portions)	$(8.51 \pm 0.75) \times 10^1$
7 (centre portion)	$(6.00 \pm 0.48) \times 10^1$
7 (end portions)	$(1.48 \pm 0.10) \times 10^2$

The results obtained for the three lanthanoids indicate that the efficiency of atomization for europium and samarium is good but that there is quite a large amount of residual terbium in the furnace after atomization. However these experiments can only be used to indicate the amount of analyte present in the furnace and other techniques have to be used to determine the type of compounds in the furnace.

3.6) COMPOUND IDENTIFICATION BY X-RAY POWDER DIFFRACTION.

Several authors have used the X-ray diffraction technique to identify the compounds present in the graphite furnace. Nickel[67] identified the reaction products and their distribution on the

graphite anode of a dc arc system. Suzuki and Ohta[68] identified sulphide in the residual material left in the furnace after heating thiourea with various elements to 573K.

In this study, x-ray powder diffraction was used to identify the compounds present in the graphite furnace prior to atomization. A known amount of either europium, samarium or terbium, as the chloride complex, was added to the furnace. After drying, the temperature was increased to 1500°C and maintained at that temperature for up to 30 seconds (the time used was concentration dependent). The furnace was then cut in half along its length and a small portion of the centre of the furnace, where the analyte was expected to be, was removed, mounted and measured by x-ray diffraction. It was found necessary to add large quantities of analyte to the furnace since initial results showed only graphite patterns. Phase analysis was carried out by the Debye-Scherrer method[69] using CuK_{α} radiation.

The major difficulty with these experiments was in obtaining a sample of the residual material since, in most cases, no residual material could be seen on the graphite surface even under magnification. The presence of carbides in the pyrolytically coated furnaces was not proved. The compounds present appeared to be the oxides but the powder patterns were very weak and these results are questionable. Initially, results for samarium in the unpyrolytically coated furnace indicated that samarium dicarbide was present however subsequent experiments indicated only the powder pattern of graphite. In the case of terbium, the residual material could be seen and collection of the sample was relatively easy. However identification of the powder diffraction pattern was more difficult. The compound present is either an unknown complex or a mixture of two compounds. It was possible to account for all the lines present on the film by taking a combination of some of the lines for terbium oxide and terbium carbide. This could be possible since there was expected to be 3.4 mg of terbium on the furnace, assuming no ashing losses, and at the graphite surface formation of terbium carbide is likely. The surface layer of terbium above this carbide may contain some of the oxide.

3.7) DISCUSSION.

Results of the previous experiments indicate that the atomization processes for the three lanthanoids investigated are quite complicated. The results of the appearance temperature experiments indicate that neither carbothermal reduction of the oxide nor volatilization of solid metal to gaseous metal are contributary processes to atom production. The accuracy of the method of determining appearance temperature is open to question but the important fact to emerge is that each of the three lanthanoids have different appearance temperatures and that these appearance temperatures are related to the relative volatilities of the individual lanthanoids.

The atomization profiles obtained are also indicative of the differences between the three lanthanoids. The atomization profile obtained for terbium using a tantalum surface is greatly improved in terms of sensitivity and peak shape. This may indicate carbide formation when a graphite surface is used. However carbide formation on pyrolytically coated graphite is unlikely and it more probable that the tantalum surface itself helps to promote the volatilization of terbium.

The results obtained from the Arrhenius type investigations are questionable especially in the low temperature regions. However, the different behaviour of terbium is again emphasised. A correlation can be made between the activation energies obtained for samarium and europium and their heats of sublimation in the high temperature region. A similar correlation was not found for terbium. The reason for this lack of correlation in the case of terbium may be incomplete atomization of the more refractory terbium even in the high temperature region due to its refractory nature. This is supported by the neutron activation results which indicate that approximately 40 per cent of the terbium remains on the furnace after atomization. These experiments suggest that the predominant atomization process is thermal dissociation of the oxide.

Carbide formation can occur, prior to atomization, but is less likely when using a pyrolytically coated furnace. However with prolonged use, the surface of the pyrolytically coated furnace may

deteriorate and carbides may then form. Therefore, it is important in the measurement of these elements that the pyrolytic coating on the furnaces is maintained.

CHAPTER 4

INTERFERENCES

4.1) INTRODUCTION.

Interference effects on samarium, europium and terbium were investigated. The effect of increasing quantities of both hydrochloric and nitric acid on the analyte response was tested. Interelement interference from the other lanthanoids and yttrium was also tested. The ratio of interferent to analyte was varied from 10 to 1 to 100 to 1 and interference was tested across the entire calibration range.

4.2) EFFECT OF INCREASING CONCENTRATIONS OF ACID.

The effect of increasing quantities of hydrochloric and nitric acids on the analyte response was tested. In a hydrochloric acid matrix, the chloride complex is usually present prior to atomization, however in a nitric acid matrix the nitrates usually thermally dissociate to the oxides. However the lanthanoid chlorides all hydrolyse to the oxychlorides on evaporation and above 1000°C these decompose to the oxide. Therefore in the case of the lanthanoids, the oxide intermediate prior to atomization can be expected in both acid media.

Optimum atomization conditions established previously were used. The hydrochloric and nitric acid concentrations were varied from 0.05 to 3.0M and 0.06 to 4.0M respectively.

For europium, increasing quantities of hydrochloric or nitric acid did not affect the atomization peak height. This suggests that the europium atomization process is not influenced by large quantities of either oxygen or hydrogen chloride gas.

For samarium, increasing quantities of hydrochloric acid did not influence the atomization peak height. Nitric acid in concentrations greater than 0.4M caused a suppression of the samarium atomization peak and at concentrations in excess of 2.0M caused a double

atomization peak.

For terbium, increasing quantities of hydrochloric acid caused a slight reduction in peak height from 0.05 to 0.5M acid above which the peak remained constant. Nitric acid caused severe suppression of the atomization peak at concentrations greater than 0.4M and at concentrations in excess of 1.0M produced a double atomization peak. (That is probably due to degradation of the graphite tubes in high acid concentration.)

At high temperatures, nitric acid decomposes to oxygen and nitrogen oxides. At low concentrations of nitric acid, these species may not affect the atomization process, however at high concentrations the excess oxygen in the system may in some way interfere with the atomization process. This interference could be due to recombination of the elemental species to form oxides in the vapour phase or the excess oxygen present may inhibit dissociation of the oxide prior to atomization. It would be expected that prior to atomization the sesquioxides would be converted to the monoxide. Although these are not stable for most of the lanthanoids, under certain conditions of temperature and pressure they may be formed. Thermodynamics would predict that terbium forms the most stable monoxide (bond dissociation energy 704 kJ/mol) followed by samarium (bond dissociation energy 587 kJ/mol) and europium (bond dissociation energy 479 kJ/mol). Therefore it seems likely that this effect would be most prominent for terbium and least prominent for europium.

4.3) INTERELEMENT INTERFERENCE.

Interference from the lanthanoids and yttrium on each of europium, samarium and terbium was established. The extent of interference was tested across the widest possible analytical range since Sen Gupta[52] mentions that interference can be overcome by dilution. (The dilution effect is commonly used to overcome interference in flame systems. The principle of this involves reduction of the total number of atoms in the light path, although the ratio of interferent to analyte does not change.)

An interferent to analyte ratio of 100, 50 and 10 to 1 was used, to establish the extent of inter-element interference, for europium, samarium and terbium. To simplify the experiments, each interferent

was added individually to the analyte since it was thought that mixtures of interferents would only serve to complicate and elongate the investigation. It was found that in the presence of the other lanthanoids it was necessary to increase the ash temperture to 1000°C for terbium and europium and to 1200°C for samarium. This did not cause a significant decrease in sensitivity for these elements in the absence of interferent.

4.3.1) Interfsrence Effects on Europium.

Interference from lanthanum, cerium, praseodynium, neodynium, samarium, gadolinium, terbium, dysprosium, holmium, erbium, thullium, ytterbium, lutetium and yttrium on the europium response was established at ratios of 100, 50 and 10 to 1 (Amounts of Eu atomized were 0.5, 1.0, 1.5, 2.0 and 2.5 ng) in each case. The effect of the interference on the analytical peak height was determined as being a percentage enhancement or suppression of the original peak (i.e. that in the absence of the interferent). A 10 per cent error margin was allowed in the measurement of analytical peaks and peaks were measured in at least duplicate.

The europium peaks were not appreciably enhanced or suppressed for the elements tested. In the presence of 100 fold excess of elements such as samarium and ytterbium, there was some peak broadening but the peak height remained within the 10 per cent error margin. However large amounts of the more refractory lanthanoids did reduce the usable life of the graphite furnace and the tube had to be replaced more frequently than usual under these conditions.

4.3.2) Interference Effects on Samarium.

Interference from lanthanum, cerium, praseodynium, neodynium, europium, gadolinium, terbium, dysprosium, holmium, erbium, thullium, ytterbium, lutetium and yttrium was established at ratios of 100, 50 and 10 to 1 (Amounts of Sm atomized were 2.5, 5.0, 7.5, 10.0 and 12.5 ng) in each case. The effect of the interferent was determined in the same manner as that of europium.

There was found to be no interference from lanthanum, cerium, praseodynium, neodynium, gadolinium, terbium, dysprosium, holmium, erbium, lutetium and yttrium at the aforementioned ratios. However at ratios of 50 and 100 to 1 europium, thullium and ytterbium caused a suppression of the analytical peak height of less than 20 per cent. The effect of the presence of europium, thullium and ytterbium on the samarium calibration curve is shown in Figure 19. As can be seen, interference can be overcome by dilution of the sample solution since at low concentrations of samarium interference is less severe. It is interesting to note that the elements which interfere in the samarium response are, like samarium, the more volatile lanthanoids. It is possible to postulate an interference mechanism based on this. If atomization of these more volatile species generates more of the element in the vapour phase then it possible that some type of mixed compound is being formed and hence less samarium exists as atoms in the vapour phase and hence is available for measurement. If atomization in all cases is due to thermal dissociation of the oxide then, perhaps, the excess quantity of oxygen present, due to the dissociation of the monoxides of thullium, ytterbium and europium, causes vapour phase recombination of samarium monoxide. Samarium monoxide is more stable than the oxides of thullium, europium and ytterbium but less stable than the oxides of the other lanthanoids.

4.3.3) Interference Effects on Terbium

Interference from lanthanum, cerium, praseodynium, neodynium, samarium, europium, gadolinium, dysprosium, holmium, erbium, thullium, ytterbium, lutetium and yttrium was established at ratios of 100, 50 and 10 to 1. 25, 50, 75, 100 and 125 ng of terbium was atomized in each case. The effect of the interferent was determined in the same manner as that of europium and samarium.

There was found to be severe interference on the terbium response from all the lanthanoids even at ratios of 10 to 1. The interference could be divided into two distinct patterns. Samarium, thullium, ytterbium and europium all caused a suppression (of less than 50 per cent) of the terbium response, an effect which increased

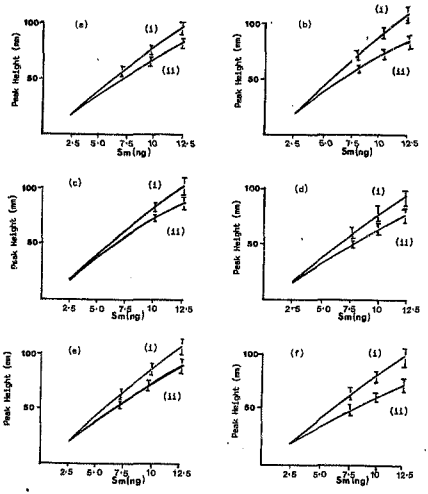

Figure 19 : Interference Effect of (a) 50 times excess Europium, (b) 100 times excess Europium, (c) 50 times excess Ytterbium, (d) 100 times excess Ytterbium, (e) 50 times excess Thullium and (f) 100 times excess Thullium on the Samarium Calibration Curve. In each case curve (i) is the samarium calibration curve and curve (ii) is the calibration in t... presence of the interferent.

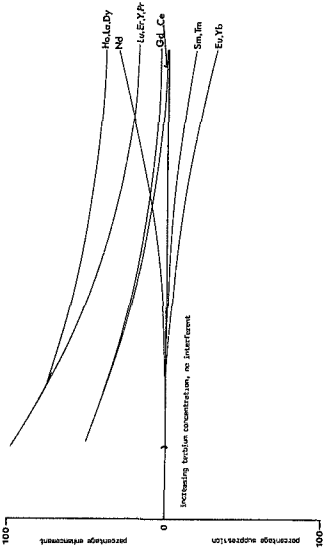

Figure 198 : Interference effect of the other lanthanoids on the terbium response. Interferent to analyte ratio, 10:1. Baseline is the terbium response in the absence of the other lanthanoids.

with increasing terbium concentration (i.e. the normal dilution effect). The other lanthanoids caused an enhancement of the terbium response which was worse at lower concentrations of terbium than at higher. In solutions containing 25 ng of terbium this effect exceeded 100 per cent enhancement in the presence of 50 fold excess of dysprosium, erbium and gadolinium. However at 125 ng terbium there was only a 50 per cent enhancement in the presence of the same interferents at the same relative concentrations.

An attempt was made to determine the interference mechanism in each of the above cases. For simplicity erbium was chosen as an example of the enhancement effect and samarium as an example of the suppressive effect.

4.3.3.1) Interference from Erbium.

In this experiment, the terbium concentration was maintained constant and the erbium concentration varied. In each case 100 ng of terbium was atomized and the amount of erbium varied from 2 to 10 000 ng. The corresponding ratios of erbium to terbium were 1 to 50, 1 to 20, 1 to 10, 1 to 1, 10 to 1, 20 to 1, 50 to 1 and 100 to 1 (i.e. from excess terbium to excess erbium). The peaks height obtained on atomization of these mixtures were compared to an atomization peak height obtained for terbium alone, a larger or smaller peak being an indication of enhancement or suppression respectively. Reproducibility was good therefore each peak was only measured in duplicate. The results of this experiment are diagrammatically represented in Figure 20. Examination of this diagram shows that ratios of erbium to terbium from 1 to 1 to 20 to 1 cause a dramatic increase in the terbium atomization peak height. Ratios of 50 to 1 and 100 to 1 (erbium to terbium) cause a decrease in the terbium response. This effect is difficult to explain but a possible explanation is that initially the addition of these lanthanoids release more terbium as the element during atomization but at higher concentrations this effect is nullified.

4.3.3.2) Interference from Samarium.

Interference effects in the presence of samarium were tested in the same manner as terbium interference. 100 ng of terbium was atomized in the presence of 2, 5, 10, 100, 1000, 2000, 5000 and

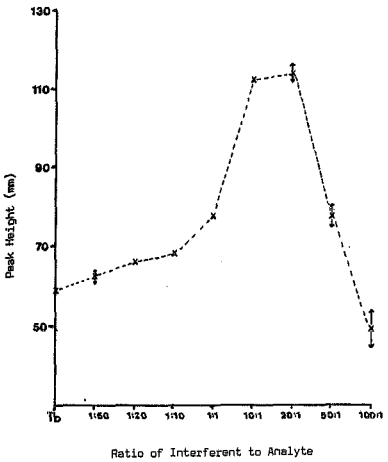

Figure 20 : Interference Effect of Erbium on Terbium at Differing Ratios of Interferent to Analyte.

10 000 ng of samarium corresponding to ratios of 1 to 50, 1 to 20, 1 to 10, 1 to 1, 10 to 1, 20 to 1, 50 to 1 and 100 to 1 (samarium to terbium). Again the atomization peak height obtained with and without samarium present was compared. In this case, an increase in the amount of samarium present caused a corresponding increase in the terbium atomization peak as shown in Figure 21. It was thought that this effect could be due to some kind of background noise or spectral overlap. Therefore these mixtures were remeasured under the same conditions except that deuterium background correction was employed. Results this time seemed to indicate that up to ratios of 1 to 1 (samarium to terbium) the terbium atomization peak height was not influenced by the samarium present. Higher quantities of samarium gave large negative, overcompensated peaks which suggests that the deuterium system could not correct for the background present. It was in fact found that varying quantities of samarium when atomized from the furnace, at the terbium wavelength and using a terbium hollow cathode lamp, exhibited calibration curve characteristics suggesting that some sort of spectral overlap is the interference effect in this case. This means that to overcome interference from samarium that the terbium and samarium would have to separated from each other.

4.4) DISCUSSION.

Different interference effects were found for each of the lanthanoids under investigation. Europium was relatively the most interference free and could easily be measured accurately in samples in the presence of even 100 fold excess of the other lanthanoids. Samarium did suffer interference from the other volatile lanthanoids at ratios of greater than 50 to 1. Therefore it would be possible to measure samarium in the presence of these other lanthanoids as long they were not in great excess. Terbium, however, is subject to severe interference from the other lanthanoids. This interference is, in some cases, due to spectral effects and in other cases to chemical effects. Therefore it would be impossible to measure terbium in samples in the presence of the other lanthanoids and it would be necessary to separate the terbium, for example by ion exchange chromatography, prior to measurement. Terbium is one of the more

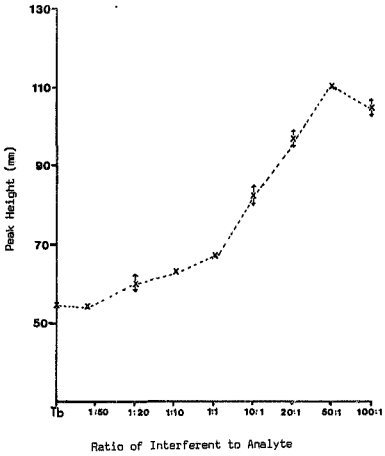

Figure 21 : Interference Effect of Samarium on Terbium at Differing Ratios of Interferent to Analyte.

refractory lanthanoids and also has a high monoxide bond dissociation energy[63].

Using the information obtained from the detailed study of these three lanthanoids it is possible to postulate some interference effects for the other lanthanoids. Ytterbium, which has a similar vapour pressure to europium (see Table 3) and monoxide bond dissociation energy[63], would also be expected to be relatively interference free. Thullium is slightly less volatile than samarium (see Table 3) but has a lower monoxide bond dissociation energy[63]. Consequently this element may be subject to similar interference effects as those of samarium. Lutetium, gadolinium, lanthanum, cerium, praseodynium and neodynium are refractory lanthanoids (see Table 3) and have high monoxide bond dissociation energies[63]. These elements may therefore be subject to interference effects similar to those experienced by terbium. This leaves the group of lanthanoids dysprosium, holmium and erbium. Their vapour pressures and monoxide bond dissociation energies lie between those of terbium and samarium therefore the interference effects will probably be less severe than those of terbium but more severe than those of samarium.

CHAPTER 5

ANALYSIS OF SAMPLES

Several samples were analysed in order to determine if an analytical method for the determination of some of the lanthanoid elements could be developed. At the beginning of this investigation, optimum conditions were established for twelve of the lanthanoids and therefore an attempt was made to determine as many of these twelve as possible in the samples. Unfortunately it was not possible to determine either praseodynium or neodynium since the hollow cathode lamps used at the beginning of this investigation were no longer available. Therefore ten of the original twelve lanthanoids; viz. samarium, europium, gadolinium, terbium, dysprosium, holmium, erbium, thullium, ytterbium and lutetium, were investigated.

5.1) SAMPLE TYPE.

The samples analysed were South African reference samples NIM 66/69 (a high grade monazite from the Rynsdorp area), NIM 39/70 (a low grade monazite from the Richards Bay area), NIM 59/70 (a medium grade monazite made by mixing one part of NIM 66/69 to two parts of NIM 39/70), NIM 18/69 (a carbonatite from South West Africa) and NIM 35/71 and 36/71 (two syenite rocks). Although recommended values are not available for all the lanthanoids in these samples, a set of preferred values for the lanthanoids in NIM 66/69, NIM 39/70 and NIM 59/70 has previously been established[70]. Furthermore these samples are used as "in-house" reference materials at the Council for Mineral Technology and the analytical results for the lanthanoid elements, although not in sufficiently large enough numbers for a statistical evaluation, have been recorded. Sen Gupta[52,53] has determined the lanthanoids in NIM 18/69, NIM 35/71 and NIM 36/71 by several techniques including flame and graphite furnace atomic absorption spectroscopy.

5.2) ANALYTICAL METHOD USED.

Several methods for the dissolution of lanthanoid containing materials are available. Sen Gupta[52,53] treated the sample with hydrofluoric, nitric and perchloric acids followed by fusion of any residual material with potassium pyrosulphate. Horsky and Fletcher[54] used repeated treatment with hydrofluoric and perchloric acids to dissolve the sample. Other methods used mainly consist of fusion techniques using a variety of fluxes.

In this investigation, the sample was fused with potassium bifluoride and leached in 10 per cent, by volume, hydrofluoric acid. Since the lanthanoid fluorides are insoluble, they are precipitated, along with any other insoluble fluorides and after digestion of the filtrate with perchloric acid, dissolved in hydrochloric acid. The accuracy of this method has been investigated at the Council for Mineral Technology[71] by the addition of a radioactive tracer ^{139}Ce to an ore prior to fusion and calculation of the amount of ^{139}Ce present in the insoluble fluoride residue. The cerium content in the precipitate was 99 per cent and since cerium fluoride is the most soluble of the lanthanoid fluorides, it can be assumed that the other lanthanoid flourides are precipitated as well.

It has been recommended by several investigators[52,54] that the lanthanoids are separated from the matrix prior to measurement by electrothermal atomization. Mazzucotelli and Frache investigated interference from the major matrix constituents on dysprosium, holmium, thullium and ytterbium[57] and recommended an ion exchange procedure[58]. Sen Gupta[52] separated and concentrated the lanthanoids by co-precipitation of their oxalates with calcium and separation of the calcium by co-precipitation of the lanthanoids with a small amount of added iron.

In this investigation, separation was effected using a cation exchange resin, Bio Rad AG50W-X8 (200 to 400 mesh). This particular resin has been used by several workers[54,58] and has been thoroughly investigated at the Council for Mineral Technology[71] for the separation of the lanthanoids from the matrix. The columns used were made of borosilicate glass and were 30 cm in length and

2 cm in internal diameter. A no.2 sintered glass disc was used as the resin support. 45ml of AG50W-X8 was placed in the column, rinsed with water and allowed to drain. The sample solution, containing 6 per cent hydrochloric acid, was added and allowed to flow through the column. The matrix impurities were eluated first with 1.85M hydrochloric acid and discarded, then the lanthanoids were eluated with 400ml of 4M hydrochloric acid. This solution was reduced to low volume on a hotplate and made up with 1 per cent hydrochloric acid for measurement by electrothermal atomization.

5.3) MEASUREMENT PROCEDURE.

Instrument conditions used for each of the lanthanoid elements were as described previously (Table 4). Furnace conditions were optimized for terbium, samarium and europium in the sample solution i.e. in the presence of the other lanthanoids. An ash temperature of 1000°C appeared to be optimum for these elements and was standardised for all the lanthanoids. The atomization temperature used in each case was 2700°C.

The concentration of lanthanoid element in each sample was determined by two methods. A calibration curve was obtained by plotting the atomization peak height versus concentration for a series of standard solutions. The concentration of lanthanoid in the sample was calculated from this graph. This method was called direct calibration. The other method used was that of analyte additions. This was carried out in the furnace itself using the analyte additions feature of the GTA-95. A constant volume of sample was pipetted onto the furnace, in each case, and varying volumes of standard solution added, the total volume pipetted onto the furnace was then adjusted to 25µl with blank solution. A graph is plotted and the concentration of lanthanoid in the sample calculated by extrapolation. This method is used when interference present in the sample causes the slope of the calibration curve to vary, however, it is not always successful in overcoming all types of interference.

Atomization peak height was measured in at least duplicate for each solution and since each sample had been prepared in duplicate, concentration should be calculated with reasonable precision.

5.4) RESULTS

The results of the analysis of these samples are tabulated in Tables 13 to 15. The "other results" used for comparison are very variable but they are the best available and very few international reference materials have recommended values for all the lanthanoids. From this comparison it appears that the lanthanoids can be divided into three distinct groups for analysis by electrothermal atomization. The first group consists of those lanthanoids which can be measured by direct calibration in most types of sample, these are samarium, europium, thullium and ytterbium (Table 13). The next group consists of those elements in which there is interference during the measurement by direct calibration but this interference can be overcome by using the analyte additions technique, these are dysprosium, holmium and erbium (Table 14). The last group consists of those elements which cannot be measured by electrothermal atomization with any real degree of precision or accuracy, these are terbium, gadolinium and lutetium (Table 15). Terbium and lutetium are each subject to severe interference in the presence of the other lanthanoids. Although the results for gadolinium in samples NIM 56/69, 39/70 and 50/71, using the standard additions technique, were comparable to the "other results", the results in NIM 18/69, 35/71 and 36/71 were not very good. Furthermore the reproducibility in the measurement of gadolinium in these samples was poor and therefore gadolinium was included in the latter group.

Table 13 : Results of Analysis of samples for Samarium, Europium, Thullium and Ytterbium.

Element	NIM 66/69			NIM 39/70			NIM 50/71			NIM 18/69			NIM 35/71			NIM 36/71		
	A	B	C	A	B	C	A	B	C	A	B	C	A	B	C	A	B	C
	µg/g	µg/g	µg/g	µg/g	µg/g	µg/g	µg/g	µg/g	µg/g	µg/g	µg/g	µg/g	µg/g	µg/g	µg/g	µg/g	µg/g	µg/g
Samarium	12.0	12.5	11.9*, 11.3, 12.1*, 12.7	18.0	18.0	16.0*, 19.0*, 22.0*, 26.0	50.0	52.0	37.0*, 52.0*, 56.0*, 43.0*, 34.0*, 19.0*, 47.0, 37.0, 53.0	183	172	185, 184, 172, 209, 224, 181, 190, 267, 250, 241, 112, 89	46	54	46, 46, 40, 50	82	92	78, 82, 82, 78
	µg/g		µg/g	µg/g		µg/g	µg/g		µg/g	µg/g	µg/g	µg/g	µg/g	µg/g	µg/g	µg/g	µg/g	µg/g
Europium	225		253*, 223*, 182, 241 527	39		43*, 46*, 26*, 40, 87	108		117*, 87*, 112, 227	65	62	43, 48, 42 43, 52, 46	12	11	14, 13	20	25	19, 23, 23
	µg/g	µg/g	µg/g	µg/g	µg/g	µg/g	µg/g	µg/g	µg/g	µg/g	µg/g	µg/g	µg/g	µg/g	µg/g	µg/g	µg/g	µg/g
Thullium	102	100	95*, 104*, 423*, 463	21	20	18*, 23*, 167*, 80	53	52	52*, 44*, 264*, 210	2.6	2.6	2.5, 3.2, 1.2, 1.2	4.1	3.2	1.9, 2.0, 3.2, 2.7	5.6	4.8	2.9, 3.4, 5.3, 4.9
	µg/g		µg/g	µg/g		µg/g	µg/g		µg/g	µg/g	µg/g	µg/g	µg/g	µg/g	µg/g	µg/g	µg/g	µg/g
Ytterbium	423		401*, 472*, 468*, 335*, 505	84		91*, 101*, 65*, 79, 98	176		181*, 176*, 185*, 193, 229	7.5	9.3	13.8, 8.6, 8.8, 8.8	12	13	14.3, 14.4 14	16.2	20	19, 19, 19

A is the result by the direct calibration method.

B is the result by the standard additions method.

C are the other results (not certified).

* Preferred values (other results are internal analysis values at NIM/GEOL).

Table 14 : Results of Analysis of samples for Dysprosium, Holmium and Erbium.

Element	NIM 68/69			NIM 39/70			NIM 50/71			NIM 18/69			NIM 38/71			NIM 36/71		
	A	B	C	A	B	C	A	B	C	A	B	C	A	B	C	A	B	C
	µg/g	µg/g	µg/g	µg/g	µg/g	µg/g	µg/g	µg/g	µg/g	µg/g	µg/g	µg/g	µg/g	µg/g	µg/g	µg/g	µg/g	µg/g
Dysprosium	3.1	2.5	3.8, 3.5*, 4.1, 3.4*, 3.0, 3.7	870	470	790*, 596, 809*, 973*, 614, 753	1.3	1.2	1.4, 1.7*, 1.9, 2.2*, 1.4, 1.2	97	66	59, 44, 55, 48	44	29	27	63	46	36, 37, 31, 21
	µg/g	µg/g	µg/g	µg/g	µg/g	µg/g	µg/g	µg/g	µg/g	µg/g	µg/g	µg/g	µg/g	µg/g	µg/g	µg/g	µg/g	µg/g
Holmium	1000	675	399*, 570*, 615*, 672	164	115	79*, 129*, 88*, 124	394	270	197*, 237*, 440*, 301	13	8.1	9.8, 10, 6.6	12	6.4	6.0, 5.2	14	9.6	7.6, 7.8, 12, 8.7
	µg/g	µg/g	µg/g	µg/g	µg/g	µg/g	µg/g	µg/g	µg/g	µg/g	µg/g	µg/g	µg/g	µg/g	µg/g	µg/g	µg/g	µg/g
Erbium	2.0	1.3	0.7*, 1.2*, 1.4*, 1.5	373	220	132*, 247*, 309*, 260	857	500	335*, 511*, 664*, 1000	43	18	21, 23, 14, 13, 32	37	16	15, 17, 12	45	24	20, 22, 31, 33

A is the result by the direct calibration method.

B is the result by the standard additions method.

C are the other results (not certified).

* Preferred results. (other results are unpublished results of analysis at NIMTEX).

Table 15 : Results of Analysis of samples for Gadolinlium, Terbium and Lutetium.

Element	NIM 06/69			NIM 39/70			NIM 50/71			NIM 18/69			NIM 38/71			NIM 38/71		
	A	B	C	A	B	C	A	B	C	A	B	C	A	B	C	A	B	C
	ng/g	ng/s	ng/s	ng/s	ng/s	ng/s	ng/s	ng/s	ng/s	ng/s		ng/s	ng/s		ng/s	ng/s		ng/s
Gadolinium	9.8	7.5	6.7, 4.1*, 8.3*, 7.2*, 8.5, 7.8	1.8	1.2	1.4*, 0.8*, 1.5*, 1.4*, 1.2, 1.3	4.4	3.5	3.2*, 1.7*, 3.4*, 3.1*, 4.0, 3.4	409		130, 134, 121, 138, 113, 95	42		26, 28, 27	-		43, 38, 80, 71
	ng/l	ng/s	ng/s	ng/s	ng/s	ng/s	ng/s	ng/s	ng/s	ng/s	ng/s	ng/s			ng/s			ng/s
Terbium	816	1574	881*, 632*, 599*, 1700*	128		163*, 128*, 280	366		368*, 299*, 200*, 723*	66	81	26, 10, 12 <17	-		9.5, 6.2, 6.7	-		9.5, 12.7, 7.6
	ng/s	ng/s	ng/s	ng/s	ng/s	ng/s	ng/s	ng/s	ng/s	ng/s	ng/s	ng/s			ng/s			ng/s
Lutetium	763	332	40*, 16*, 89* 47	129	80	10*, 4*, 8.8	304	222	14*, 9.7* 21	99	21	4.2, <0.9 <18	-	-	4.2, <2.6	-	-	4.2, <2.6

A is the result by the direct calibration method.

B is the result by the standard additions method.

C are the other results (not certified).

* Preferred values [10]. (other results are intralaboratory analytical results i.e. BELGATOM).

CHAPTER 6

CONCLUSIONS

The measurement of selected lanthanoid elements by electrothermal atomization atomic absorption spectroscopy has been investigated.

Optimum ash and atomization temperatures have been established for twelve of the lanthanoids viz. neodynium, praseodynium, samarium, europium, gadolinium, terbium, dysprosium, holmium, erbium, thullium, ytterbium and lutetium. Calibration curves and precision of measurement have also been established.

Terbium, samarium and europium were investigated in more detail. These elements were chosen because initial investigation indicated that during atomization from the furnace they exhibited different volatilization characteristics from each other.

Attempts were made to determine the atomization processes using a variety of techniques. Results of these tests indicated that samarium and europium were similar in atomization behaviour but that terbium had quite different atomization characteristics. However it is thought that in each case atomization is primarily the result of thermal dissociation of a monoxide intermediate. Terbium would be expected to form the most stable monoxide and experimental observation confirms that atomization of terbium is more difficult than the other study elements.

Interference effects on the three lanthanoids were tested. Interference from increasing concentrations of hydrochloric and nitric acids was quantified. Interference was most severe in the case of terbium but the samarium response was also suppressed by excess concentrations of nitric acid. This is probably a direct result of the increase in the amount of oxygen present in the furnace due to thermal dissociation of the nitric acid. Interelement interferences were also established. Interference effects were tested at selected analyte concentrations, for interferent to analyte ratios of 10, 50 and 100 to 1. There was no interference on the europium response. There was a supression of the samarium response from excess europium,

ytterbium and thullium. This was thought to be a chemical interference due to recombination in the vapour phase. However this interference could be overcome by dilution since interference was more severe a high concentrations of samarium. In the case of terbium, interference was severe and could not be overcome so easily. All the other lanthanoids either suppressed or enhanced the terbium response to some degree. For erbium this was found to be a chemical effect and in small concentrations erbium actually acted as a releasing agent for terbium. In the case of samarium, interference was found to be spectral. Interference on terbium therefore is not easily overcome and some sort of separation of the terbium from the other lanthanoids would be necessary prior to measurement.

An attempt was then made to measure the lanthanoids in selected rock samples. Certified reference materials with recommended values for all the lanthanoids were not available therefore six "in-house" reference materials, which have been extensively analysed at Mintek, were used. These samples were fused with potassium bifluoride then the lanthanoids were separated from the matrix by ion exchange. Results obtained indicated that the lanthanoids could be split into three groups, in terms of their analysis, in this type of material. The first group consisted of those elements for which the analysis was relatively uncomplicated - these were samarium, europium, ytterbium and thullium. The second group consisted of those elements for which analysis using the method of analyte additions was necessary - these were holmium, erbium and dysprosium. Finally, the last group consisted of those elements for which interference was too severe to allow measurement with any degree of accuracy - these were terbium, lutetium and gadolium.

REFERENCES

1. International Union of Pure and Applied Chemistry "Nomenclature of Inorganic Chemistry.", second edition, Butterworths, London. 1970

2. Gscheidner, K.A. "Industrial Applications of Rare Earth Elements." American Chemical Society, Washington D.C. 1981

3. Gschneidner, K.A. and Eyring, L. "Handbook of the Physics and Chemistry of the Rare Earths." Vol. 1, North Holland Publishing Company, 1978, New York.

4. Weltz, B. "Atomic Absorption Spectroscopy" Verlag Chemie, Weinheim, New York. 1976

5. Kirk and Othmer "Encyclopedia of Chemical Technology" vol. 18 John Wiley and Sons, New York. 1984

6. Comprehensive Inorganic Chemistry. vol. 4 , Pergamon Press. 1973. pp. 1-105

7. Dana, J.W. "A System of Mineralogy." John Wiley and Sons, New York. 1920

8. Read, H.H. "Rutley's Elements of Mineralogy" Thomas Murby and Co., London. 1947

9. Spedding, F.H. and Daane, A.H."The Rare Earths." John Wiley and Sons. 1961. New York.

10 Hultgren, R. et al "Selected Values of the Thermodynamic Properties of the Elements." American Society for Metals, Ohio. 1973

11. Pannish, M.B. Jnl. of Chem. Phys. vol. 34. 1961. pp. 2197-2198

12. Walsh, P.W., Goldstein, H.W. and White, D. Jnl. of Am. Cer.Soc. vol. 43, no. 5. 1960. pp. 229-233

13. Haschke, J.M. and Eick, H.A. J. Phys. Chem. vol.72, no.2. 1968. pp.1697-1702

14. Walsh, A., Spectrochim Acta. vol.7. 1955. pp.108-117

15. Kirkbright, G.F. and Sargent, M. "Atomic Absorption and Fluorescence Spectroscopy." Academic Press Inc., London. 1974

16. Ebdon, L. "An Introduction to Atomic Absorption Spectroscopy" Heydon and Son Ltd., London. 1982

17. Fuller, C.W. "Electrothermal Atomization for Atomic Absorption Spectrometry." Analytical Science Monographs, The Chemical Society, London. 1977

18. King, A.S., Astrophys. J. vol. 21. 1905. p. 236

19. King, A.S., Astrophys. J. vol. 27. 1908. p. 353

20. L'vov, B.V., J. Eng. Phys. (USSR) vol. 2. 1959. p. 44

21. Massman, H., Z. Anal. Chem. vol. 225. 1967. p. 203

22. Massman, H., Spectrochim. Acta vol.23B. 1968. p. 215

23. Manning, D.C. and Ediger, R.D. Atomic Absorption Newsletter vol. 15, part 2. 1976. pp. 42-44

24. L'vov, B.V. and Pelieva, L.A. Canadian Journal of Spectroscopy vol. 23, no. 1. 1978. pp.1-4

25. Suzuki, M. and Ohta, K. Prog. Analyt. Atom. Spectrosc. vol. 6. 1983. pp.49-162

26. Fritzsche, H., Wegschneider, W., Knapp, G. and Ortner, H.M. Talanta vol. 26. 1979. pp. 219-226

27. Loos-Vollebregt, M.T.C, De Galan, L., Uffelen, J.W.M., Slavin, W.and Manning, D.C. Spectrochim. Acta vol. 38B, no. 5/6. 1983. pp.799-807

28. Van dan Broek, W.M.G.T. et al Anal. Chim. Acta vol. 100. 1978. pp 121-138

29. L'vov, B.V. "Atomic Absorption Spectrochemical Analysis" Adam Hilger, London. 1970.

30. Torsi, G. and Tessari, G. Anal Chem vol. 45, no. 11. 1973. pp.1812-1816

31. Fuller, C.N. Analyst vol. 99. 1974. pp739-744

32. International Union of Pure and Applied Chemistry Spectrochim. Acta vol. 33B. 1978. pp.261-264

33. Gucer, S. and Massman, H. Proc. 17th Coll. Spectrosc. Int. Florence, vol. 1. 1973. p51

34. Massman, H. and Gucer, S. Spectrochim. Acta vol. 29B. 1974. pp.283-300

35. Amas, M.D., Bennett, P.A., Brodie, K.G., Lung, P.W.Y. and Matousek, J.P. Anal. Chem. vol. 43. 1971. pp 211-215

36. Frech, W. and Cedergren, A. Anal. Chim. Acta vol. 82. 1976. pp. 93-102

37. Kirkbright, G.F.K. and Snook, R.D. Anal. Chem. vol. 51, no. 12. 1979. pp. 1938-1941

38. Batley, E.G. and Matousek, P.J. Anal. Chem. vol. 52. 1980. pp. 1570-1574

39. Fairless, C. and Bard, A.J. Anal. Chem. vol. 45. 1973. pp. 2289-2291

40. Jensen, F.O., Dolezal, J. and Langmyhr, F.J. Anal. Chim. Acta vol. 72. 1974. pp. 245-250

41. Newton, M.P. and Davis, O.G. Anal. Chem. vol. 47. 1975. pp. 2003-2009

42. Lund, W. and Larsen, B.V. Anal. Chim. Acta vol. 81. 1976. pp. 319-324

43. Sotera, J.J. and Khan, H.L. American Laboratory vol. 14, pt. 2. 1982. pp.100-108

44. Koirtyohann, S.R and Pickett, E.E. Anal. Chem. vol. 37. 1965. pp. 601-603

45. de Loos-Vollebregt, M.T.C. and de Galan, L. Spectrochim. Acta vol. 33B. 1969. pp. 495-511

46. Smith, S.B. Jr. and Hieftje, G.M. Applied Spectroscopy vol. 37, no. 5. 1983. pp. 419-424

47. Sturgeon, R.E. and Chakrabarti, C.L. Anal. Chem vol. 49. 1977. pp. 90-97

48. Churella, D.J. and Copeland, T.R. Anal. Chem. vol. 50. 1978. pp. 309-314

49. Sturgeon, R.E. and Berman, S.S. Anal Chem vol. 53. 1981. pp. 832-839

50. Fuavao, V.A. and Sneddon, J. Atomic Spectrosc. vol. 4, no. 5. 1983. pp. 179-181

51. Grobenski, Z. Fresenius Z Anal. Chem. vol. 289. 1978. pp. 337-345

52. Sen Gupta, J.G. Talanta vol. 28. 1980. pp. 31-36

53. Sen Gupta, J.G. Geostandards Newsletter vol. 6, no. 2. 1982. pp. 241-248

54. Horsky, S.J. and Fletcher, W.K. Chemical Geology vol. 32. 1981. pp. 335-340

55. L'vov, B.V. and Pelieva, L.A. Cn. Jnl. of Spectrosc. vol. 23, no. 1. 1978. pp.1-4

56. Mazzucotelli, A. and Frache, R. Mikrochim. Acta II. 1981. pp. 323-328

57. Mazzucotelli, A., Galli, M. and Frache, R. Analyst vol. 107. 1982. pp. 104-109

58. Mazucotelli, A. and Frache, R. Analyst vol. 105. 1980. pp. 497-501

59. Rothery, E. "Analytical Methods for Graphite Tube Atomizers" Varian Techtron Pty., Australia. 1982

60. Campbell, W.C. and Ottoway, J.M. Talanta vol. 21. 1974. pp. 837-844

61. Sturgeon, R.E., Chakrabarti, C.L. and Langford, C.H. Anal. Chem. vol. 48, no. 12. 1976. pp 1792-1807

62. Sastry, M.D., Shide, M.K., Savitri, K., Babu, Y. and Joshi, B.D. Fresenius Z Anal. Chem. vol. 298. 1979. pp. 367-372

63. Pedley, J.B. and Marshall, E.M. Jnl. Phys. Chem. Ref. Data. vol. 12, no. 4. 1983. p. 985

64. Gebelt, R.E. and Eick, H.A. Jnl. Chem. Phys. vol. 44, no. 8. 1966. pp 2872-26

65. Haschke, J.M. and Daline, T.A. Jnl. Chem. Thermodynamics vol. 14. 1982. pp. 1019-1028

66. Filby, E.E. and Ames, L.L. Jnl. Phys. Chem. vol. 75, no. 6. 1971. pp. 848-854

67. Nickel, H. Spectrochim. Acta vol. 238. 1968. pp. 323-343

68. Suzuki, M. and Ohta, K. Anal. Chim. Acta vol. 151. 1983. pp. 401-407

69. Lipson, H. and Steele, H. "Interpretation of X-Ray Powder Diffraction Patterns" Macmillan and Co. Ltd., London. 1970

70. Stoch, H., Steele, T.W. and Copelowitz, I. "The Establishment of Preferred Values for a Series of Rare Earth Samples." National Institute for Metallurgy, Report No. 1807, 1976

71. Jones, E.A., Watson, A.E. and Dixon, K. "The Separation and Determination of Trace and Minor Amounts of Individual Rare Earths in Silicates." National Institute for Metallurgy, Report No. 1422, 1972. Randburg